Predicting Census Survey Response Rates via Interpretable Nonparametric Additive Models with Structured Interactions

Shibal Ibrahim* Rahul Mazumder[†] Peter Radchenko[‡] Emanuel Ben-David[§]
August, 2021

Abstract

Accurate and interpretable prediction of survey response rates is important from an operational standpoint. The US Census Bureau's well-known ROAM application uses principled statistical models trained on the US Census Planning Database data to identify hard-to-survey areas. An earlier crowdsourcing competition revealed that an ensemble of regression trees led to the best performance in predicting survey response rates; however, the corresponding models could not be adopted for the intended application due to limited interpretability. In this paper, we present new interpretable statistical methods to predict, with high accuracy, response rates in surveys. We study sparse nonparametric additive models with pairwise interactions via ℓ_0 -regularization, as well as hierarchically structured variants that provide enhanced interpretability. Despite strong methodological underpinnings, such models can be computationally challenging – we present new scalable algorithms for learning these models. We also establish novel non-asymptotic error bounds for the proposed estimators. Experiments based on the US Census Planning Database demonstrate that our methods lead to high-quality predictive models that permit actionable interpretability for different segments of the population. Interestingly, our methods provide significant gains in interpretability without losing in predictive performance to state-of-the-art black-box machine learning methods based on gradient boosting and feedforward neural networks. Our code implementation in python is available at https: //github.com/ShibalIbrahim/Additive-Models-with-Structured-Interactions.

1 Introduction

Context and background. Sample surveys and censuses are primary data sources in social science studies. However, low and often unpredictable response rates in surveys remain a continual source of concern [Erdman and Bates, 2016, Smith, 2014, Tourangeau et al., 2014]. Tourangeau et al. [2014] discuss a multitude of factors that make parts of the population hard-to-survey – such factors are often used to improve sampling strategies, questionnaire designs, recruitment methods, and the language in which the interview is conducted, among others. Erdman and Bates [2016] emphasize the usefulness of having an indicator for hard-to-survey areas to guide targeted surveying (including oversampling), staff recruitment strategies, and targeted follow-ups for non-responders. For major campaigns such as the decennial US Census, this approach can help guide resource allocation for advertisements and building community partnership activities. Eliciting responses from non-self-responding households through nonresponse follow-up operations can be very costly and time consuming. The Census Bureau estimates that a single percentage increase in the self-response rate amounts to roughly 85 million

^{*}MIT Department of Electrical Engineering and Computer Science. email: shibal@mit.edu

[†]MIT Sloan School of Management, Operations Research Center and MIT Center for Statistics. email rahulmaz@mit.edu

 $^{^{\}ddagger}$ University of Sydney. email: peter.radchenko@sydney.edu.au

[§]United States Census Bureau. email: emanuel.ben.david@census.gov

dollars saved in personal follow-up costs [US Census Bureau, 2009, Bates and Mulry, 2011]. Apart from the cost, the quality of proxy enumerations and imputations is typically significantly lower than that of self-responses [Mule, 2012].

Both the UK Office for National Statistics and the US Census Bureau have created measures that help quantify the difficulty in gathering data across different geographic areas [Erdman and Bates, 2016]. Bruce et al. [2001] of the US Census Bureau introduced a hard-to-count (HTC) score for identifying difficult to enumerate segments of the population. The HTC score, which is based on 12 carefully chosen covariates (for example, housing variables and socio-demographic/economic indicators) has found its use in the planning for the 2010 Census and many other national surveys. The HTC score, however, has some limitations and was later improved to the low-response-score, or LRS [Erdman and Bates, 2016]. The LRS plays a key role in the US Census Bureau's Response Outreach Area Mapper (ROAM) application to identify hard-to-survey areas. The LRS appears to have been partly motivated by the 2012 nationwide competition, organized by the Census Bureau in partnership with Kaggle, on predicting the mail-return rates [Erdman and Bates, 2016]. This competition aimed to solicit models that were highly predictive of the decennial census response rates, easily replicable, inherently interpretable, and consistent for the use in the field at various levels of geography [Erdman and Bates, 2016]. Even though the winning models from the competition had good predictive performance, they lacked reproducibility and interpretability. Some of the winning models included covariates that are not publicly available; in particular, they were not chosen from within the US Census Bureau Planning Database. Additionally, as pointed out by Erdman and Bates [2016], the winning models included covariates that were good predictors but not actionable². Interpretability suffered due to a multitude of factors. First, the winning models were based on complex ensemble methods (for example, random forests and gradient boosting). Second, these methods employed a large number of covariates (the best model had nearly 340), which hurt the model parsimony. After careful analysis, Erdman and Bates [2016] proposed a linear model based on 25 covariates to define the LRS. While this model suffered in terms of predictive accuracy compared to the black-box machine learning methods, it was highly interpretable and led to useful actionable insights.

The purpose of this paper is to propose well-grounded nonparametric statistical models that are interpretable and have good predictive performance, so that they can be used to complement the LRS. We seek to create statistical models with strong theoretical underpinnings that lend operational insights into factors that influence self-response rates in surveys. This, in particular, can facilitate the goal of having a census that is cost effective and results in improved coverage.

Our methodological contributions. Our key methodological contributions can be summarised as follows: (i) we propose a new family of estimators based on nonparametric additive models with interactions under combinatorial constraints, to promote parsimony and interpretability; (ii) we establish novel statistical guarantees for the resulting estimators; and (iii) we present large-scale algorithms to obtain high-quality solutions for our proposed learning tasks, significantly expanding the current computational landscape for nonparametric additive models. Next, we provide an overview of these contributions.

Statistical models. Our statistical estimators are based on Additive Models [Hastie and Tibshirani, 1987, Hastie et al., 2001], or AMs, with smooth nonlinear components that include nonlinear pairwise interactions between covariates. Given response $y \in \mathbb{R}$ and feature-vector $\mathbf{x} := (x_1, \dots, x_p) \in \mathbb{R}^p$, we model the conditional mean function as

$$\mathbb{E}(y|\mathbf{x}) = \sum_{j \in [p]} f_j(x_j) + \sum_{j < k} f_{j,k}(x_j, x_k),$$
(1)

¹https://www.census.gov/library/visualizations/2017/geo/roam.html

²These include covariates such as the nearest neighboring block group return rates and margins of error for various estimates. Models that incorporate such features are not actionable.

where f_j and $f_{j,k}$ are unknown smooth univariate and bivariate functions, respectively³. Drawing inspiration from linear model settings [Bach et al., 2012], we propose new methodology to estimate the unknown functional components via an optimization problem with structural constraints arising from interpretability considerations. To obtain a model with few predictors, that is, with many of the components $\{f_j\}$ and $\{f_{j,k}\}$ estimated as exactly zero, we consider a novel ℓ_0 -regularized approach⁴, penalizing the number of nonzero components in the model. In addition, we explore a refined notion of interpretability in the context of interaction modeling – namely, hierarchical sparsity – inspired by its usage in the context of linear models [Hazimeh and Mazumder, 2020b, Bien et al., 2013]. To our knowledge, this is the first exploration of combinatorially structured statistical models in the context of nonparametric modeling.

Statistical error bounds. We present non-asymptotic oracle prediction error bounds for our proposed estimator. While bounds of this type have been established for sparse nonparametric additive models with main effects, we are not aware of any similar existing bounds for nonparametric models with pairwise interactions. An appealing aspect of our theory is that it allows for model misspecification, avoiding the popular but impractical assumption of a ground truth sparse additive model. Our results apply to the high-dimensional setting where the number of predictors is large and are of independent interest in the context of high-dimensional nonparametric function estimation under sparsity constraints.

Large-scale computation. The estimators we consider here can be formulated as mixed integer programming (MIP) problems [Wolsey and Nemhauser, 1999]. Significant advances in algorithms and software for MIP (for example, Gurobi, Cplex, Mosek) over the past several years [Bertsimas et al., 2016] make it an attractive computational tool. With n observations and p features, and using splines with K knots for every component, the MIP encouraging sparsity in all main effects and pairwise interactions has an objective involving a squared error part with p-terms and a penalty part with p-terms. The optimization is done over p-many continuous and p-many binary variables. This poses formidable computational challenges for problem-instances p-to p-many scalable algorithms. To obtain good solutions at scale, we use techniques inspired by first order methods in continuous optimization [Nesterov, 2003] and a careful exploitation of the problem-structure. For the problem with hierarchical interactions, we present a relax-and-round based strategy, that appears to work well in our applications.

Related Work. There is an impressive body of methodological and theoretical work on using convex ℓ_1 -based approaches to fit sparse AMs without interactions [see, for example, Meier et al., 2009, Ravikumar et al., 2009, Huang et al., 2010, Koltchinskii and Yuan, 2010, Zhao and Liu, 2012, Yuan and Zhou, 2016, and the references therein]. Even with main-effects alone, these convex optimization-based methods face computational challenges for the problem-scales we seek to address⁵. This prevents a potential user from realizing the full potential of AMs in large-scale settings that arise in many practical applications in the modern-day world. In terms of statistical properties, the ℓ_0 -based estimators can offer improvements over their ℓ_1 -counterparts. Recent work [Hazimeh et al., 2021] studies the ℓ_0 -regularized framework for variable selection in AMs without interactions. In the presence of interactions, which is the focus herein, the problem of variable selection with AMs becomes considerably more challenging. Incorporating hierarchically structured interactions brings additional nuances. To the best of our knowledge, our algorithmic framework for sparse AMs with interactions is novel and

³We assume functions $\{f_j\}$ and $\{f_{j,k}\}$ are twice continuously differentiable with square-integrable second derivatives. ⁴For recent examples of such approaches in the context of linear regression, see Bertsimas et al. [2016], Mazumder and Radchenko [2017], Mazumder et al. [2017], Hazimeh and Mazumder [2020a] and the references therein.

⁵Based on our experience, currently available software (for example, R package SAM) encounters numerical difficulties for instances where n is on the order of thousands, and p is on the order of hundreds.

is likely to be of independent interest from a computational methodology perspective in applications beyond the one studied herein.

Applied Contributions. While our methodological contributions are broadly applicable, we focus on the performance of our proposal on the Census application that motivates our study. Our empirical results on the Planning Database show that our framework leads to improved prediction of the response rates when compared to the currently used methods based on linear regression [Erdman and Bates, 2016]. At the same time, our nonlinear models are substantially more compact, using 8-20 times fewer interaction effects than the corresponding linear models. Interestingly, the prediction accuracy of our interpretable models is comparable to that of black-box machine learning methods such as neural networks and XGBoost. We interpret our models to gather deeper operational insights into what factors influence response rates in surveys, and how the predictions vary across different segments of the population.

Organization. Section 2 presents the different statistical models pursued in this paper. Section 3 investigates the statistical properties of our proposed estimators. Section 4 discusses how to obtain solutions to the corresponding large-scale discrete optimization problems. Section 5 discusses numerical results for the US Census Bureau application that motivates this study. Proofs of the theoretical results and additional experiment details are provided in the supplement.

2 Statistical Models and Methodology

In this section we present the different models we consider in this paper. Section 2.1 gives an overview of additive models with nonlinear main effects and pairwise interactions; it also provides an optimization formulation for the estimation procedure. Section 2.2 presents our new models to incorporate sparsity in the main and interaction effects. Section 2.3 discusses a novel structured variant that obeys the principle of strong hierarchy.

2.1 Additive models: nonlinear main-effects and pairwise interactions

Given data $\{(y_i, \mathbf{x}_i)\}_1^n$, our key objective is to learn a multivariate conditional mean function $f(\mathbf{x}) := \mathbb{E}(y|\mathbf{x})$, where $f: \mathbb{R}^p \mapsto \mathbb{R}$ is an unknown smooth function [Wahba, 1990]. It is well known that such functions become difficult to estimate even for moderately high p due to the curse of dimensionality, therefore we will focus on a smaller class of models corresponding to additive structures [Hastie and Tibshirani, 1987, Stone, 1986]. A popular approach considered in the literature estimates a nonparametric additive model containing main-effects only, with $f(\mathbf{x}) = \sum_{j=1}^p f_j(x_j)$, where each f_j is an unknown univariate smooth function of the j-th coordinate in \mathbf{x} , namely x_j . In various applications, however, additive models based on main-effects alone may not lead to a sufficiently rich representation for predicting the outcome of interest: including interaction terms can lead to better predictive models that still remain interpretable to a practitioner [Hastie et al., 2001, Hastie and Tibshirani, 1987]. Learning interpretable linear models with interactions is a fundamental problem in statistical modeling, with widespread applications in medical sciences and healthcare, e-commerce applications, recommender system problems, and sentiment analysis, among others [Bien et al., 2013, Hastie et al., 2015].

The importance of incorporating interaction effects when predicting the self-response rate has been highlighted in the Census report by Erdman and Bates [2016], even though the authors focus on a linear model with main effects only (i.e., with no interactions). Indeed, our exploratory analysis suggests that many of the features provided in the US Census Bureau Planning Database dataset typically "interact" to predict the response. For example, there is interaction between the percentage of people who do not speak English well and the percentage of renters in the area. In areas with relatively high concentration of poor English speakers ($\geq 5.4\%$), the self-response rate decreases at the rate of 0.33%

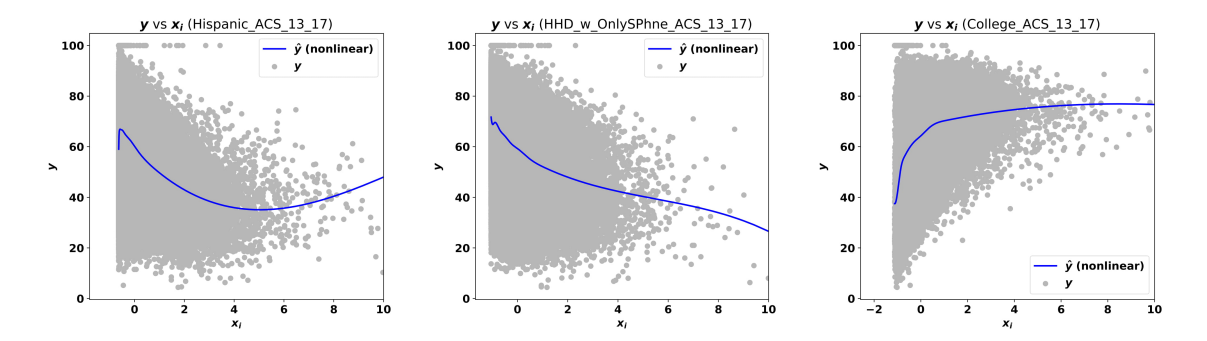


Figure 1: Panels [Left]-[Right] illustrate marginal nonparametric fits for the self-response rate output variable versus three covariates. Each marginal fit, displayed on a scatter plot with a solid blue line, clearly suggests a nonlinear relationship of the output vs the individual covariate (we note that the covariates are standardized.) The x-axis corresponds to: [Left] Persons of Hispanic Origin in the ACS; [Middle] Number of households that have only a smartphone and no other computing device; [Right] Persons 25 years and over with college degree or higher in the ACS.

for a unit increase in renters percentage. On the other hand, when the concentration of poor English speakers is relatively low ($\leq 1.6\%$), the self-response rate decreases at the rate of 0.21%. Similarly, there is a strong interaction effect between covariates "single unit households" and "moved 5 Years ago" in terms of predicting the low self-response rate.

An additive model with nonlinear main effects and pairwise interactions extends the traditional AM framework with main effects alone [Hastie et al., 2001, Radchenko and James, 2010], and is given by model (1), where the unknown components $\{f_j\}_j$ and $\{f_{j,k}\}_{j,k}$ need to be estimated from the data. This leads to two key challenges. The presence of $O(p^2)$ -many unknown nonparametric functions results in statistical challenges even for a moderate value of p. Additional regularization (for example, in the form of sparsity in the components) may be necessary to obtain a reliable statistical model with good generalization properties – this is addressed in Sections 2.2 and 2.3. Furthermore, as we mention in Section 1, estimating model (1) leads to severe computational challenges for large problems (for example, those with $n \approx 10^5$ and $p^2 \approx 10^5$, similar to the instances we consider in our applications) – this is addressed in Section 4.

We assume that the components $\{f_j\}$ and $\{f_{j,k}\}$ are smooth (for example, twice continuously differentiable). For illustration, consider Figure 1, which shows that the marginal fits for the self-response rate appear to be well-approximated by smooth nonlinear functions. Using squared ℓ_2 -loss as the data fidelity term, the task of learning model (1) can be expressed as the following infinite dimensional optimization problem:

$$\min_{\substack{f_j \in \mathcal{C}_1, \forall j \\ f_{j,k} \in \mathcal{C}_2, \forall j < k}} \frac{1}{n} \sum_{i \in [n]} \left(y_i - \sum_{j \in [p]} f_j(x_{ij}) - \sum_{j < k} f_{j,k}(x_{ij}, x_{ik}) \right)^2 + \lambda \left[\sum_{j \in [p]} \Omega(f_j) + \sum_{j < k} \Omega(f_{j,k}) \right], \quad (2)$$

where the main-effects $f_j \in \mathcal{C}_1$ for all j and the interaction effects $f_{j,k} \in \mathcal{C}_2$ for all (j,k); with \mathcal{C}_1 , \mathcal{C}_2 denoting the sets of smooth functions in 1D and 2D respectively. Above, Ω is a roughness penalty measuring the smoothness level⁶ of components f_j and $f_{j,k}$ and $\lambda \geq 0$ is a regularization parameter controlling the smoothness of the functions. Below, we present a reformulation of (2) as a finite-dimensional quadratic program. Before presenting this reformulation, we first discuss optimization formulations for learning each of the building blocks: the one-dimensional main effects and the two dimensional interaction effects.

 $^{^6 \}text{For example, } \Omega(f_j) = \int f_j''(x_j)^2 dx_j \text{ and } \Omega(f_{ij}) = \int_{x_j x_k} (\partial^2 f_{j,k}/\partial x_j^2)^2 + (\partial^2 f_{j,k}/\partial x_j \partial x_k)^2 + (\partial^2 f_{j,k}/\partial x_k^2)^2 dx_j dx_k.$

2.1.1 Understanding the building blocks: one and two dimensional fits.

We discuss how the individual main effects and interaction effects, can be estimated via quadratic optimization.

One dimensional nonparametric function estimation. Suppose that we have observations $\{(y_i,u_i)\}_1^n$ corresponding to a univariate response y_i and a univariate predictor $u_i \in [0,1]$. If the underlying relationship between y and u can be modeled via a twice continuously differentiable (i.e., smooth) function m(u), we can estimate m(u) as a function that minimizes the following objective: $\sum_{i=1}^n (y_i - m(u_i))^2 + \lambda \int (m''(u))^2 du$. This functional optimization problem can be reduced to a finite dimensional quadratic program by using a suitable basis representation for m(u). For example, if all of the u_i 's are distinct and $b_1(u), \ldots, b_n(u)$ are the basis functions [for example, cubic splines with knots at the observations u_i , Wahba, 1990, Hastie et al., 2015], then we can write $m(u) = \sum_{i=1}^n \gamma_i b_i(u)$. In this case, $\int (m''(u))^2 du = \gamma^{\mathsf{T}} \mathbf{D} \gamma$, where \mathbf{D} is a positive semidefinite matrix with the (i, l)-th entry given by $\int b_i''(u)b_l''(u)du$.

Instead of using an n-dimensional basis representation for m(u), which is computationally expensive and perhaps statistically redundant, one can choose a smaller number of basis functions, such as $K = O(n^{1/5})$; this leads to a low-rank representation of \mathbf{D} [Hall and Opsomer, 2005, Li and Ruppert, 2008] and hence an improved computational performance. Reducing the number of basis elements from n to K leads to fewer parameters at the expense of a marginal increase in bias [Wahba, 1990], which is often negligible in practice.

The evaluations of the function m(u) at the n data points can be stacked together in the form of a vector $\mathbf{B}\boldsymbol{\beta}$, where \mathbf{B} is an $n \times K$ matrix of basis functions evaluated at the observations, and $\boldsymbol{\beta} \in \mathbb{R}^K$ contains the corresponding basis coefficients that need to be estimated from the data. The univariate function fitting problem then reduces to a regularized least squares problem given by $\min_{\boldsymbol{\beta} \in \mathbb{R}^K} \{ \|\boldsymbol{y} - \boldsymbol{B}\boldsymbol{\beta}\|_2^2 + \lambda \boldsymbol{\beta}^T \boldsymbol{A}\boldsymbol{\beta} \}.$

While many choices of spline bases are available [Wood, 2006, Hastie et al., 2001], we use penalized B-splines for their appealing statistical and computational properties. Following Eilers and Marx [1996], a second-order finite difference penalty on the coefficients of adjacent B-splines serves as a good discrete approximation to the integral of the squared second-order derivative penalty Ω discussed above. The regularized least squares problem takes the form

$$\min_{\beta} \| \boldsymbol{y} - \boldsymbol{B}\boldsymbol{\beta} \|_{2}^{2} + \lambda \sum_{l=1}^{K-2} (\Delta^{2} \beta_{l})^{2},$$
 (3)

where K is the number of the B-spline basis functions and $\Delta^2 \beta_l = \beta_l - 2\beta_{l+1} + \beta_{l+2}$ is the second-order finite difference of the coefficients of adjacent B-splines with equidistant knots. We note that the regularization term can be represented in matrix form as $\lambda \| \mathbf{D} \boldsymbol{\beta} \|_2^2$, where $\mathbf{D} \in \mathbb{R}^{(K-2)\times K}$ is a banded matrix with nonzero entries given by $d_{l,l} = 1$, $d_{l,l+1} = -2$ and $d_{l,l+2} = 1$ for $l \in [K-2]$.

Two dimensional nonparametric function estimation. To model the response as a function of two covariates one can again use reduced rank parameterizations, in the form of multivariate splines [Wahba, 1990], thin-plate splines [Kammann and Wand, 2003], or tensor products of B-splines [Eilers and Marx, 2003, Wood, 2006], for example. We use tensor products of B-splines to model the two-dimensional smooth functions of the form m(u,v), with $(u,v) \in [0,1]^2$ for concreteness. We start from a low-rank B-spline basis representation for the marginal smooth functions as $m_1(u) = \sum_{k=1}^K \beta_k b_k(u)$ and $m_2(v) = \sum_{l=1}^L \delta_l c_l(v)$, where $\{b_k\}$ and $\{c_l\}$ are B-spline basis functions, and $\{\beta_k\}$, $\{\delta_l\}$ are unknown basis coefficients. We convert the marginal smooth function m_1 into a smooth function of covariates u and v by allowing the coefficients β_k to vary in a smooth fashion with respect to v. Given that we have an available basis for representing smooth functions of v, we can write $\beta_k(v) = \sum_{l=1}^L \delta_{k,l} c_l(v)$ and then arrive at the tensor smooth given by $m(u,v) = \sum_{k=1}^K \sum_{l=1}^L \delta_{k,l} b_k(u) c_l(v)$. We note that

the evaluations of the function m(u,v) at the n data points can be stacked together in a vector written as $\mathbf{R}\gamma$. We denote the vectors evaluating the two marginal functional bases, $\{b_k(\cdot)\}$ and $\{c_l(\cdot)\}$, at the i-th data point as $\mathbf{B}_i \in \mathbb{R}^K$ and $\mathbf{C}_i \in \mathbb{R}^L$, respectively. In matrix notation, the model matrix $\mathbf{R} \in \mathbb{R}^{n \times KL}$ can be expressed as $\mathbf{R} = (\mathbf{B} \otimes \mathbf{1}_L) \odot (\mathbf{1}_K \otimes \mathbf{C})$, where operations \otimes and \odot denote Kronecker product and element-wise multiplication respectively. The basis coefficients $\delta_{k,l}$ are appropriately ordered into the vector $\mathbf{\gamma} \in \mathbb{R}^{KL}$ via the vectorization operation $\mathbf{\gamma} = \text{vec}(\mathbf{\delta}) = [\delta_{1,1}, \cdots, \delta_{K,1}, \delta_{1,2}, \cdots, \delta_{K,2}, \cdots, \delta_{1,L}, \cdots, \delta_{K,L}]^{\top}$, where $\mathbf{\delta} = [\delta_{k,l}]_{k \in [K], l \in [L]}$ stores the basis coefficients in matrix form.

The smooth 2D estimate can be obtained by making use of tensor products and a discretized version of the smoothness penalty [Eilers and Marx, 2003], given by:

$$\min_{\gamma} \|\boldsymbol{y} - \boldsymbol{R}\gamma\|_{2}^{2} + \lambda_{b} \sum_{k=1}^{K} \sum_{l=1}^{L-2} (\Delta_{(1)}^{2} \delta_{k,l})^{2} + \lambda_{c} \sum_{l=1}^{L} \sum_{k=1}^{K-2} (\Delta_{(2)}^{2} \delta_{k,l})^{2},$$
(4)

where $\Delta_{(1)}^2 \delta_{k,l} = \delta_{k,l} - 2\delta_{k,l+1} + \delta_{k,l+2}$ and $\Delta_{(2)}^2 \delta_{k,l} = \delta_{k,l} - 2\delta_{k+1,l} + \delta_{k+2,l}$. The regularization terms above can be compactly represented as quadratic forms in γ as follows:

$$\min_{\boldsymbol{\gamma}} \|\boldsymbol{y} - \boldsymbol{R}\boldsymbol{\gamma}\|_{2}^{2} + \lambda_{b}\boldsymbol{\gamma}^{T}\boldsymbol{P}_{b}\boldsymbol{\gamma} + \lambda_{c}\boldsymbol{\gamma}^{T}\boldsymbol{P}_{c}\boldsymbol{\gamma}, \tag{5}$$

where $P_b = (D^T D) \otimes I_L$ and $P_c = I_K \otimes (D^T D)$. The regularizer ensures that the coefficients in the same row (or column) of δ vary regularly, leading to a smooth 2D surface.

2.1.2 Additive model with interactions.

The one-dimensional and two-dimensional building blocks allow us to parametrize model (1) using a finite basis representation. Let $\mathbf{f}_j = (f_j(x_{1j}), \dots, f_j(x_{nj}))$ and $\mathbf{f}_{j,k} = (f_{j,k}(x_{1j}, x_{1k}), \dots, f_{j,k}(x_{nj}, x_{nk}))$ denote the evaluations of the main effect component f_j and the interaction component $f_{j,k}$, respectively, at the n data points. Then, $\mathbf{f}_j = \mathbf{B}_j \boldsymbol{\beta}_j$, where $\mathbf{B}_j \in \mathbb{R}^{n \times K_j}$ is the model matrix and $\boldsymbol{\beta}_j \in \mathbb{R}^{K_j}$ is the vector of coefficients for each main effect component. Similarly, $\mathbf{f}_{j,k} = \mathbf{B}_{j,k} \boldsymbol{\theta}_{j,k}$, where $\mathbf{B}_{j,k} \in \mathbb{R}^{N \times K_{j,k}}$ is the model matrix and $\boldsymbol{\theta}_{j,k} \in \mathbb{R}^{K_{j,k}}$ is the vector of coefficients for each interaction effect component. Here, K_j and $K_{j,k}$ denote the corresponding dimensions of the bases – in our implementation, all the values K_j are taken to be the same and all the $K_{j,k}$ are taken to be the same as well.

The smoothness penalties discussed in the Supplement for the 1D and 2D cases are imposed on each main effect and interaction component, respectively. Writing β for the vector obtained by stacking together the coefficients β_j , $j \in [p]$ for the main-effects, and defining the vector $\boldsymbol{\theta}$ for the interaction effects analogously, we express the optimization problem (2) as follows:

$$\min_{\boldsymbol{\beta},\boldsymbol{\theta}} g_{\lambda_1}(\boldsymbol{\beta},\boldsymbol{\theta}) \stackrel{\text{def}}{=} \frac{1}{n} \left\| \boldsymbol{y} - \left[\sum_{j \in [p]} \boldsymbol{B}_j \boldsymbol{\beta}_i + \sum_{j \le k} \boldsymbol{B}_{j,k} \boldsymbol{\theta}_{j,k} \right] \right\|_2^2 + \lambda_1 \left[\sum_{j \in [p]} \boldsymbol{\beta}_j^T \boldsymbol{S}_j \boldsymbol{\beta}_j + \sum_{j \le k} \boldsymbol{\theta}_{j,k}^T \boldsymbol{S}_{j,k} \boldsymbol{\theta}_{j,k} \right].$$
(6)

Here, $S_j = D_j^T D_j$ and $S_{j,k} = (D_j^T D_j) \otimes I_k + I_j \otimes (D_k^T D_k)$ are the smoothness penalty matrices for the main effects and the interaction components, respectively. In (6), for convenience, we use the same smoothness penalty λ_1 for both the main and the interaction effects.

2.2 Parsimonious models via ℓ_0 -penalization

We seek to limit the number of main and interaction effects in our model – both for statistical reasons (to mitigate overfitting in the presence of a large number of parameters) and for interpretability reasons (a compact model is easier to interpret and lends better operational insights than a dense one) – this aligns with the *bet on sparsity* principle advocated in Hastie et al. [2001].

While a significant amount of impressive work has been devoted towards studying sparsity in the context of linear models, sparsity in nonlinear models has received less attention. Interestingly, we

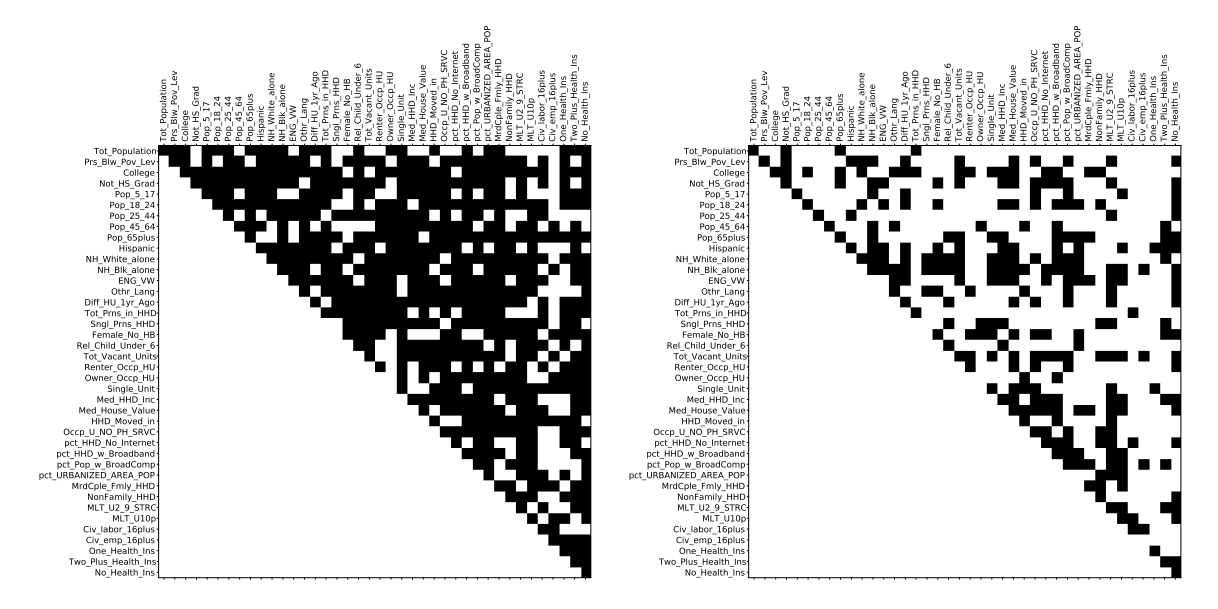


Figure 2: Sparsity pattern of the main and interaction effects presented in a $p \times p$ matrix: a black square on the diagonal indicates the presence of a main effect, and an off-diagonal black square indicates the presence of an interaction effect in the joint model. [Left] Panel illustrates the sparsity pattern of a Lasso model with main and interaction effects. [Right] Panel illustrates the sparsity pattern of a nonlinear model with main and interaction effects, i.e., model (7). Both models were trained on a 2019 US Census Bureau Planning Database dataset (predicting the tract-level self-response rate) with p=40 covariates and 74,000 samples. Nonlinear models lead to much more compact and hence, easier to interpret models compared to linear models.

observe that the notion of parsimony is linked to the model being used and changes, for example, depending on whether we use a linear interaction model of the form $\mathbb{E}(y|\mathbf{x}) = \sum_j x_j \beta_j + \sum_{j < k} x_j x_k \beta_{jk}$ or model (1) that has nonlinear components. For motivation, we consider Figure 2, which presents our findings on a 2019 US Census Bureau Planning Database dataset with 40 covariates⁷. These include covariates used for the low-response-score [Erdman and Bates, 2014], important covariates highlighted in Appendix C of the 019 US Census Bureau Planning Database Documentation US Census Bureau [2019], plus some additional covariates capturing internet penetration and urbanization. Specifically, we observe that:

- The more general *nonlinear* approach with interactions⁸ results in a substantially more compact model (with few nonzero components) than the linear model with interactions.
- The out-of-sample prediction accuracy of this nonlinear model is superior compared to its linear model counterpart.

The above observation suggests that the nonlinear model with sparse interactions may be preferable over its linear model counterpart. While the above discussion is based on a smaller dataset with p = 40 features, our findings generally carry over to the expanded dataset, as discussed in Section 5.

To obtain an additive model with a small number of main and interaction effects, we consider the following estimator:

$$\min_{\boldsymbol{\beta},\boldsymbol{\theta}} G(\boldsymbol{\beta},\boldsymbol{\theta}) \stackrel{\text{\tiny def}}{=} g_{\lambda_1}(\boldsymbol{\beta},\boldsymbol{\theta}) + \lambda_2 \Big[\sum_{j \in [p]} \mathbb{1} \big[\boldsymbol{\beta}_j \neq \mathbf{0} \big] + \alpha \sum_{j < k} \mathbb{1} \big[\boldsymbol{\theta}_{j,k} \neq \mathbf{0} \big] \Big], \tag{7}$$

⁷These covariates were selected based on discussions with researchers at the US Census Bureau.

⁸This corresponds to an estimate available from (7). We present the model leading to the best prediction performance on the validation set – see Section 5 for details.

where $\mathbb{1}[\cdot]$ is an indicator function, λ_2 controls the number of components selected, and $\alpha \in [1,\infty)$ controls the tradeoff between the number of main effects and the number of interaction effects in the model. Note that Problem (7) can be formulated as a MIP, and hence can be solved to optimality with modern commercial solvers (for example, Guorbi, Mosek) for small/moderate scale problems. Another possibility is to consider tailored nonlinear branch-and-bound techniques following Hazimeh et al. [2020]. Since we intend to compute solutions to (7) for a family of tuning parameters (λ_1, λ_2) at scale, it is more practical to consider approximate solutions as discussed in Section 4.1. Once a good (approximate) solution to (7) is available, we can employ MIP techniques to improve the solution and/or certify the quality of the solution, extending the local search techniques presented in Hazimeh and Mazumder [2020a] for the sparse linear regression problem. To our knowledge, this the first work to pursue a methodological investigation of estimator (7).

Related Work. The combinatorial optimization problem (7) is NP-hard. Several methodological approaches have been proposed to address convex relaxations of (7) when no interactions are present. These are based on variants of group-Lasso type formulations – see, for example, Ravikumar et al. [2009], Zhao and Liu [2012], Meier et al. [2009], Buhlmann and van de Geer [2011]. Hazimeh et al. [2021] considers ℓ_0 -formulations for the setting without interaction effects and demonstrates the merits of using ℓ_0 -based formulations over convex relaxation-based approaches.

Despite the appeal of formulation (7), computational challenges appear to be a key limiting factor in exploring the usefulness of this model in applications arising in practice. A principal goal of our paper is to advance the computational frontiers of (7) – Section 4 provides further details.

2.3 Sparse nonparametric interactions under strong hierarchy

Problem (7) limits the total number of main and interaction effects and works well in our experiments (see Section 5 for the details) in terms of obtaining a sparse model with good predictive performance. In terms of variable selection properties, however, (7) can lead to the inclusion of an interaction effect, say, $\{(j,k)\}\$ where at least one of the corresponding main-effects $\{j\}$ or $\{k\}$ is excluded from the model. This may be somewhat problematic from an interpretation viewpoint. Hence, it may be desirable to enforce additional constraints in (7), imposing the so-called hierarchy constraints [McCullagh and Nelder, 1989, Bien et al., 2013. Here, we consider the well-known strong hierarchy constraint, where an interaction effect $\{(j,k)\}$ is included in the model only if the corresponding main effects are also included. In addition to improved interpretation, strong hierarchy can reduce the effective number of features in the model, which in turn can reduce the operational costs associated with data collection Bien et al., 2013, Hazimeh and Mazumder, 2020b.

To enforce strong hierarchy into model (7), we consider the following estimator:

$$\min_{\boldsymbol{\beta},\boldsymbol{\theta}} \quad g_{\lambda_1}(\boldsymbol{\beta},\boldsymbol{\theta}) + \lambda_2 \Big[\sum_{j \in [p]} \mathbb{1}[\boldsymbol{\beta}_j \neq \mathbf{0}] + \alpha \sum_{j < k} \mathbb{1}[\boldsymbol{\theta}_{j,k} \neq \mathbf{0}] \Big]$$
s.t.
$$\boldsymbol{\theta}_{j,k} \neq \mathbf{0} \implies \boldsymbol{\beta}_j \neq \mathbf{0} \quad \& \quad \boldsymbol{\beta}_k \neq \mathbf{0} \quad \forall j < k, \ j \in [p], \ k \in [p].$$
(8a)

s.t.
$$\boldsymbol{\theta}_{j,k} \neq \mathbf{0} \implies \boldsymbol{\beta}_j \neq \mathbf{0} \& \boldsymbol{\beta}_k \neq \mathbf{0} \quad \forall j < k, \ j \in [p], \ k \in [p].$$
 (8b)

We note that (8) differs from (7) in the additional strong hierarchy constraint appearing in (8b). By using binary variables to model sparsity in the main/interaction effects and to encode the hierarchy constraint (8b), Problem (8) can be expressed as the following MIP:

$$\min_{\boldsymbol{\beta},\boldsymbol{\theta},\boldsymbol{z}} g_{\lambda_{1}}(\boldsymbol{\beta},\boldsymbol{\theta}) + \lambda_{2} \left[\sum_{j \in [p]} z_{j} + \alpha \sum_{j < k} z_{j,k} \right]$$
s.t. $z_{j} \in \{0,1\}, \quad \|\boldsymbol{\beta}_{j}\|_{2} \leq Mz_{j} \quad \forall j \in [p]$

$$z_{j,k} \in \{0,1\}, \quad \|\boldsymbol{\theta}_{j,k}\|_{2} \leq Mz_{j,k} \quad \forall j < k,$$

$$z_{j,k} \leq z_{j}, \quad z_{j,k} \leq z_{k}, \quad \forall j < k,$$
(9)

⁹In terms of existing implementations, R package SAM presents specialized algorithms for a convex relaxation of (7) without interactions. SAM would not run on the dataset we consider here.

where the BigM parameter M is a sufficiently large finite constant such that an optimal solution to (9) satisfies $\max_j \|\boldsymbol{\beta}_j\|_2 \leq M$ and $\max_{j,k} \|\boldsymbol{\theta}_{j,k}\|_2 \leq M$. Binary variable z_j (as well as $z_{j,k}$) indicates whether the corresponding main effect $\boldsymbol{\beta}_j$ (respectively, interaction effect $\boldsymbol{\theta}_{j,k}$) is zero or not; the constraint appearing in the last line of (9) enforces the hierarchy constraint in (8b).

To our knowledge, this is the first work to study estimator (9). The methodology presented here is of independent interest in the context of structured nonparametric learning with interactions. In Section 4, we discuss computational challenges associated with (8) and propose scalable algorithms to obtain good solutions for this problem.

Related Work. Methodology for strong hierarchy in linear models has been studied in the statistics/machine learning literature [Bien et al., 2013, Lim and Hastie, 2015, Yan and Bien, 2017, Hazimeh and Mazumder, 2020b] – these works appear to focus on the linear setting, which is more restrictive than the nonlinear setting we consider here. Radchenko and James [2010] consider hierarchy constraints in the nonparametric setting, via convex optimization schemes. As far as we know, current techniques are unable to scale to the functional learning instances we consider in our paper.

3 Statistical Theory

In this section, we explore statistical error bounds of our proposed estimator in the deterministic design setting. The proofs of all the established results are provided in the Supplement. Given a candidate regression function $f:[0,1]^p \to \mathbb{R}$ of the form $f(\mathbf{x}) = \sum_{j \in [p]} f_j(x_j) + \sum_{j < k} f_{j,k}(x_j, x_k)$, we define its sparsity level as

$$G(f) = \sum_{j \in [p]} \mathbb{1}[\mathbf{f}_j \neq \mathbf{0}] + \sum_{j < k} \mathbb{1}[\mathbf{f}_{j,k} \neq \mathbf{0}].$$

To ensure identifiability of the additive representation for $f(\mathbf{x})$ additional restrictions need to be imposed on the components f_j and $f_{j,k}$. For the simplicity of the presentation, we avoid specifying a particular set of restrictions and treat every representation of f as equivalent, with the understanding that one particular representation is used when evaluating quantities such as G(f).

We write $\|\cdot\|_{L_2}$ for the L_2 norm of a real-valued function on $[0,1]^2$ or [0,1]. We focus on the case where \mathcal{C}_1 and \mathcal{C}_2 are L_2 -Sobolev spaces. More specifically, we let

$$C_2 = \left\{ g(u,v) : [0,1]^2 \mapsto \mathbb{R}, \ \|g\|_{L_2} + \left\| \frac{\partial^2 g}{\partial u^2} \right\|_{L_2} + \left\| \frac{\partial^2 g}{\partial u \partial v} \right\|_{L_2} + \left\| \frac{\partial^2 g}{\partial v^2} \right\|_{L_2} < \infty \right\}$$

$$\Omega(g) = \left\| \frac{\partial^2 g}{\partial u^2} \right\|_{L_2}^2 + \left\| \frac{\partial^2 g}{\partial u \partial v} \right\|_{L_2}^2 + \left\| \frac{\partial^2 g}{\partial v^2} \right\|_{L_2}^2,$$

and also let $C_1 = \{h : [0,1] \mapsto \mathbb{R}, \|h\|_{L_2} + \|h''\|_{L_2} < \infty\}, \quad \Omega(h) = \|h''\|_{L_2}^2$. We define the corresponding space of additive functions with interactions as

$$\mathcal{C}_{\text{gr}} = \{ f : [0,1]^p \mapsto \mathbb{R}, \ f(\mathbf{x}) = \sum_{j \in [p]} f_j(x_j) + \sum_{j < k} f_{j,k}(x_j, x_k), \ f_j \in \mathcal{C}_1, \ f_{j,k} \in \mathcal{C}_2, \ G(f) \le K \},$$

where K is some arbitrarily large universal constant, and let

$$\Omega_{\rm gr}(f) = \sum_{j \in [p]} \Omega(f_j) + \sum_{j < k} \Omega(f_{j,k}).$$

We associate each $f \in \mathcal{C}_{gr}$ with the vector $\mathbf{f} = \sum_{j \in [p]} \mathbf{f}_j + \sum_{j < k} \mathbf{f}_{j,k}$, where $\mathbf{f}_j = (f_j(x_{1j}), ..., f_j(x_{nj}))$ and $\mathbf{f}_{j,k} = (f_{j,k}(x_{1j}, x_{1k}), ..., f_{j,k}(x_{nj}, x_{nk}))$.

We write $\|\cdot\|_n$ for the Euclidean norm divided by \sqrt{n} and focus on the estimator that solves the ℓ_0 -penalized version of optimization problem (2), that is

$$\widehat{f} = \underset{f \in \mathcal{C}_{gr}}{\operatorname{arg\,min}} \|\mathbf{y} - \mathbf{f}\|_n^2 + \lambda_n \Omega_{gr}(f) + \mu_n G(f). \tag{10}$$

We assume that the observed data follows the model $\mathbf{y} = \mathbf{f}^* + \boldsymbol{\epsilon}$, where $\mathbf{f}^* = \left(f(\mathbf{x}_1), ..., f(\mathbf{x}_n)\right)$ is the vector representation of a function $f^* : [0,1]^p \mapsto \mathbb{R}$, and the elements of $\boldsymbol{\epsilon}$ are independent $N(0,\sigma^2)$ with $\sigma>0$. We refer to $\|\hat{\mathbf{f}}-\mathbf{f}^*\|_n^2$ as the prediction error for estimator \hat{f} . We write $r_n = n^{-1/3}$, noting that r_n^2 is the optimal prediction error rate in the bivariate regression setting where $f^* \in \mathcal{C}_{\mathrm{gr}}$. We say that a constant is *universal* if it does not depend on other parameters, such as n or p. We use the notation \gtrsim and \lesssim to indicate that inequalities \geq and \leq , respectively, hold up to positive universal multiplicative factors.

Theorem 1 presented below derives a general non-asymptotic oracle prediction error bound, comparing the performance of our estimator to that of sparse approximations to the true regression function. Bounds of this type have been established for sparse nonparametric additive models with main effects; however, we are not aware of similar existing bounds for nonparametric models with pairwise interactions. The existing work has focused mainly on the Lasso-based estimators, which encourage sparsity in the main-effects by penalizing the magnitudes of the functional components [see Meier et al., 2009, Koltchinskii and Yuan, 2010, Tan and Zhang, 2019, and the references therein]. The use of ℓ_1 -based relaxations, in lieu of ℓ_0 -penalization, to induce sparsity in the main-effects can lead to unwanted shrinkage, which may interfere with variable selection. The approach in Hazimeh et al. [2021] controls the number of main-effects directly, demonstrating the benefits of ℓ_0 -regularization both theoretically and empirically. In our theoretical development, we consider an ℓ_0 -based approach to penalize the number of both main and pairwise interaction effects. We note that our analysis focuses on the ℓ_0 -penalized formulation, which poses additional theoretical challenges relative to the ℓ_0 -constrained formulation. To our knowledge, the error bounds established here in the context of sparse nonparametric AMs with pairwise interactions are novel.

The following result corresponds to the high-dimensional setting where p is large (Remark 2 below addresses the classical fixed p case), hence the stated error bound holds with high probability.

Theorem 1. There exists a universal constant c_1 , such that if $\lambda_n \geq c_1 \sigma \left[r_n^2 + r_n \sqrt{\log(ep)/n} \right]$, then

$$\|\widehat{\mathbf{f}} - \mathbf{f}^*\|_n^2 + \lambda_n \Omega_{\mathrm{gr}}(\widehat{f}) + \mu_n G(\widehat{f}) \lesssim \inf_{f \in \mathcal{C}_{gr}} \left[\|\mathbf{f} - \mathbf{f}^*\|_n^2 + \lambda_n \Omega_{\mathrm{gr}}(f) + \mu_n G(f) \right] + \sigma^2 \left[r_n^2 + \frac{\log(ep)}{n} \right]$$

with probability at least 1 - 1/p.

We note that a popular approach in the literature, even in the linear setting, has been to assume a sparse underlying model for the data. In contrast, Theorem 1 does not assume a ground truth sparse additive model, allowing for model misspecification and incorporating the approximation error into the bound. This feature is especially appealing for our application of interest where the ground truth is not available. The following corollary complements the general result in Theorem 1 by establishing a non-asymptotic prediction error bound for the proposed approach in the case where the additive model is correctly specified.

Corollary 1. Suppose that $f^* \in \mathcal{C}_{gr}$. There exist universal constants c_1 and c_2 , such that if $\lambda_n \geq c_1 \sigma \left[r_n^2 + r_n \sqrt{\log(ep)/n} \right]$ and $\mu_n \geq c_2 \sigma^2 \left[r_n^2 + \log(ep)/n \right] + c_2 \lambda_n \Omega_{gr}(f^*)$, then

$$\|\widehat{\mathbf{f}} - \mathbf{f}^*\|_n^2 \lesssim \sigma^2 \left[r_n^2 + \frac{\log(cp)}{n} \right] + \lambda_n \Omega_{gr}(f^*) + \mu_n G(f^*) \quad and \quad G(\widehat{f}) \leq G(f^*)$$
 (11)

with probability at least 1 - 1/p.

We make the following observations about the established results.

Remark 1. Inequality (11) yields the following prediction error bound:

$$\|\widehat{\mathbf{f}} - \mathbf{f}^*\|_n^2 \lesssim \sigma^2 \left[n^{-2/3} + \frac{\log(ep)}{n} \right]. \tag{12}$$

In contrast to the Lasso-based estimators for nonparametric additive models [for example, Meier et al., 2009, Tan and Zhang, 2019], the above error rate holds without imposing assumptions on the design. The accompanying sparsity bound $G(\hat{f}) \leq G(f^*)$ is exact, and hence stronger than the corresponding bounds for the Lasso-based estimators [for example, Lounici et al., 2011]. The latter bounds hold up to a multiplicative constant, which depends on the design and can be significantly greater than one. When $\log(p) \lesssim n^{1/3}$, the prediction error rate in (12) matches the optimal bivariate rate of $n^{-2/3}$.

Remark 2. Theorem 1 and Corollary 1 are stated for the high-dimensional setting, where p is large. We show in the proof of Corollary 1 that in the classical asymptotic setting, where p is fixed and n tends to infinity, an appropriate choice of λ_n and μ_n leads to the optimal bivariate rate of convergence, $\|\hat{\mathbf{f}} - \mathbf{f}^*\|_n^2 = O_p(n^{-2/3})$, and the exact sparsity bound $G(\hat{f}) \leq G(f^*)$ that holds with probability tending to one.

Remark 3. The proof of Theorem 1 establishes a somewhat more general result by replacing the second derivative in the definition of C_{gr} and Ω_{gr} with an m-th derivative and redefining r_n as $n^{-m/(2m+2)}$. The corresponding prediction error bound extends the result in Theorem 2 of Lin and Zhang [2006], which is established for the fixed p setting, from the main effects models to the interaction models. When $\log(p) \lesssim n^{1/(m+1)}$, the prediction error rate matches the optimal bivariate rate of $n^{-m/(m+1)}$.

4 Efficient Computations at Scale

We present specialized algorithms to obtain solutions to Problems (7) and (8). Our approach scales to instances with $n \approx 10^5$ and $p \approx 500$ (with approx. 10^5 interaction effects). Using 25 knots for every component, this leads to estimating around 2.5 million basis coefficients.

Current state-of-art. To appreciate the computational challenges of sparse nonlinear additive models with interactions, and nonparametric additive models in general, we provide a few examples of the problem instances that can be handled by current state-of-the-art algorithms with publicly available implementations. Current implementations based on R package SAM [Zhao and Liu, 2012], the stepwise GAM function in R package step.gam (which performs greedy variable selection), and Python package pyGAM, take on the order of days to run and/or face numerical difficulties for instances with $n \approx 10^5$ to obtain a single solution without interactions. Furthermore, pyGAM is unable to do automated variable selection. Wood et al. [2017] present an interesting approach for AMs that scales to large n settings (see R package mgcv) but is unable to perform automated variable selection in the presence of a large number of features (Wood et al., 2017 report instances containing fewer than 20 pre-specified main and interaction effects).

4.1 Algorithms for sparse nonlinear interactions: Problem (7)

As mentioned earlier, (7) can be expressed as a MIP and solved for small-to-moderate scale problems using modern MIP solvers. However, given the problem-sizes of interest and the fact that we seek to compute solutions to (7) for a family of tuning parameters, we discuss faster alternatives. We note that the objective in Problem (7) is a sum of a smooth convex loss function and a discontinuous regularizer separable across the components $\{\beta_j\}$ and $\{\theta_{i,k}\}$. Motivated by the strong empirical performance of cyclical coordinate descent (CD) methods [Wright, 2015] in ℓ_0 -penalized linear regression [Hazimeh and Mazumder, 2020a], we explore block CD methods to obtain fast approximate solutions for the nonparametric setting with interactions (7). For convergence guarantees of this procedure, see Hazimeh and Mazumder [2020a] and references therein.

4.1.1 Cyclic Block Coordinate Descent (CD).

In our block CD method, the blocks correspond to the basis coefficients for either the main effects $\{\boldsymbol{\beta}_j\}_j$ or the interaction effects $\{\boldsymbol{\theta}_{j,k}\}_{j,k}$. Given an initialization $(\boldsymbol{\beta}_1^{(0)}, \dots, \boldsymbol{\beta}_p^{(0)}, \boldsymbol{\theta}_{1,2}^{(0)},$

 $\cdots, \boldsymbol{\theta}_{p-1,p}^{(0)}$), at every cycle, we sequentially sweep across the main effects and the interaction effects. If we denote the solution after t cycles by $(\boldsymbol{\beta}_1^{(t)}, \cdots, \boldsymbol{\beta}_p^{(t)}, \boldsymbol{\theta}_{1,2}^{(t)}, \cdots, \boldsymbol{\theta}_{p-1,p}^{(t)})$, then the block of coefficients for j-th main effect $\boldsymbol{\beta}_j^{(t+1)}$ at the cycle t+1 is obtained by optimizing (7) with respect to $\boldsymbol{\beta}_j$, with other variables held fixed:

$$\boldsymbol{\beta}_{j}^{(t+1)} \in \underset{\boldsymbol{\beta}_{j} \in \mathbb{R}^{K_{j}}}{\operatorname{arg \, min}} G(\boldsymbol{\beta}_{1}^{(t+1)}, \cdots, \boldsymbol{\beta}_{j-1}^{(t+1)}, \boldsymbol{\beta}_{j}, \boldsymbol{\beta}_{j+1}^{(t)}, \cdots, \boldsymbol{\beta}_{p}^{(t)}, \quad \boldsymbol{\theta}_{1,2}^{(t)}, \cdots, \boldsymbol{\theta}_{p-1,p}^{(t)}). \tag{13}$$

Similarly, $\boldsymbol{\theta}_{i,k}^{(t+1)}$, the coefficients for the (j,k)-th interaction effect at cycle t+1 is updated as

$$\boldsymbol{\theta}_{j,k}^{(t+1)} \in \underset{\boldsymbol{\theta}_{j,k} \in \mathbb{R}^{K_{j,k}}}{\min} G(\boldsymbol{\beta}_{1}^{(t+1)}, \cdots, \boldsymbol{\beta}_{p}^{(t+1)}, \quad \boldsymbol{\theta}_{1,2}^{(t+1)}, \cdots, \boldsymbol{\theta}_{(j,k)-1}^{(t+1)}, \boldsymbol{\theta}_{j,k}, \boldsymbol{\theta}_{(j,k)+1}^{(t)}, \cdots, \boldsymbol{\theta}_{p-1,p}^{(t)}). \tag{14}$$

The block minimization problem (13) reduces to:

$$\boldsymbol{\beta}_{j}^{(t+1)} = \underset{\boldsymbol{\beta}_{i} \in \mathbb{R}^{K_{j}}}{\min} \ \psi_{j}(\boldsymbol{r}^{(t)}; \boldsymbol{\beta}_{j}) := \frac{1}{n} \|\boldsymbol{r}^{(t)} - \boldsymbol{B}_{j} \boldsymbol{\beta}_{j}\|_{2}^{2} + \lambda_{1} \ \boldsymbol{\beta}_{j}^{T} \boldsymbol{S}_{j} \boldsymbol{\beta}_{j} + \lambda_{2} \cdot \mathbb{1}[\boldsymbol{\beta}_{j} \neq \boldsymbol{0}], \tag{15}$$

where $\mathbf{r}^{(t)} = \mathbf{y} - (\sum_{j'=1}^{j-1} \mathbf{B}_{j'} \boldsymbol{\beta}_{j'}^{(t+1)} + \sum_{j'=j+1}^{p} \mathbf{B}_{j'} \boldsymbol{\beta}_{j'}^{(t)} + \sum_{j' < k'} \mathbf{B}_{j',k'} \boldsymbol{\theta}_{j',k'}^{(t)})$ denotes the residual. A solution to (15) can be computed in closed form via the following thresholding operator:

$$\boldsymbol{\beta}_j^{(t+1)} = \begin{cases} \mathbf{0} & \text{if } \psi_j(\boldsymbol{r}^{(t)}; \mathbf{0}) \leq \min_{\boldsymbol{\beta}_j \neq \mathbf{0}} \psi_j(\boldsymbol{r}^{(t)}; \boldsymbol{\beta}_j) \\ \left(\boldsymbol{B}_j^T \boldsymbol{B}_j + n \lambda_1 \boldsymbol{S}_j\right)^{-1} \boldsymbol{B}_j^T \boldsymbol{r}^{(t)} & \text{otherwise.} \end{cases}$$

Similarly, the sub-problem for the interaction effects is

$$\boldsymbol{\theta}_{j,k}^{(t+1)} = \underset{\boldsymbol{\theta}_{j,k} \in \mathbb{R}^{K_{j,k}}}{\operatorname{arg \, min}} \psi_{j,k}(\boldsymbol{r}^{(t)}; \boldsymbol{\theta}_{j,k}) := \frac{1}{n} \|\boldsymbol{r}^{(t)} - \boldsymbol{B}_{j,k} \boldsymbol{\theta}_{j,k}\|_{2}^{2} + \lambda_{1} \|\boldsymbol{\theta}_{j,k}^{T} \boldsymbol{S}_{j,k} \boldsymbol{\theta}_{j,k} + \alpha \lambda_{2} \cdot \mathbb{1}[\boldsymbol{\theta}_{j,k} \neq \boldsymbol{0}], \quad (16)$$

where $\mathbf{r}^{(t)} = \mathbf{y} - (\sum_{j'=1}^{p} \mathbf{B}_{j'} \boldsymbol{\beta}_{j'}^{(t+1)} + \sum_{(j',k')=1,2}^{(j,k)-1} \mathbf{B}_{j',k'} \boldsymbol{\theta}_{j',k'}^{(t+1)} + \sum_{(j',k')=(j,k)+1}^{p-1,p} \mathbf{B}_{j',k'} \boldsymbol{\theta}_{j',k'}^{(t)})$. A solution to this problem is given by

$$\boldsymbol{\theta}_{j,k}^{(t+1)} = \begin{cases} \mathbf{0} & \text{if } \psi_{j,k}(\boldsymbol{r}^{(t)}; \mathbf{0}) \leq \min_{\boldsymbol{\theta}_{j,k} \neq \mathbf{0}} \psi_{j,k}(\boldsymbol{r}^{(t)}; \boldsymbol{\theta}_{j,k}) \\ (\boldsymbol{B}_{j,k}^T \boldsymbol{B}_{j,k} + N\lambda_1 \boldsymbol{S}_{j,k})^{-1} \boldsymbol{B}_{j,k}^T \boldsymbol{r}^{(t)} & \text{otherwise.} \end{cases}$$
(17)

These block CD updates need to be paired with several computational devices in the form of active set updates, cached matrix factorizations, and warm-starts, among others. We draw inspiration from similar strategies used in CD-based procedures for sparse linear regression [Hazimeh and Mazumder, 2020a, Friedman et al., 2010], and adapt them to our problem. We discuss some of these below.

4.1.2 Scalability considerations

Active set updates A main computational bottleneck in the block CD approach is the number of passes across the $O(p^2)$ blocks. However, as we anticipate a solution that is sparse (with few nonzero main and interaction effects), we use an active set strategy. We restrict our block CD procedure to a small subset Q of the $O(p^2)$ variables, with all blocks outside the active set being set to zero. Once the CD algorithm converges on the active set, we check if all blocks outside the active set satisfy

the coordinate-wise optimality conditions¹⁰. If there are any violations, we select the corresponding blocks, append them to the current active set, and then rerun our block CD procedure. As there are finitely many active sets, the algorithm is guaranteed to converge – in practice, with warm-start continuation (discussed below), the number of active set updates is quite small, and the algorithm is found to converge quite quickly.

Cached matrix factorizations The updates (13) and (14) require computing a matrix inverse. In particular, if a block is nonzero, we need to compute a linear system solution of the form: $A_l^{-1}b_l$ where $A_l = B_l^T B_l + n\lambda_1 S_l$. We note that matrix A_l is fixed throughout the CD updates and is independent of the choice of the sparsity regularization parameter λ_2 – hence, we pre-compute a matrix factorization for A_l (for example, an LU decomposition) and use it to compute the solution to the linear system. As the dimension of A_l equals the number of basis coefficients, which is small, this can be done quite efficiently.

Warm-starts We use our CD procedure to compute a path of solutions to (7) for a 2D grid of tuning parameters $(\lambda_1, \lambda_2) \in \{\lambda_1^{(l)}\}_{l=0}^L \times \{\lambda_2^{(m)}\}_{m=0}^M$, where λ_1 corresponds to the smoothness parameter and λ_2 the sparsity parameter. Here, $\lambda_1^{(l)} > \lambda_1^{(l+1)}$ for all l, and $\lambda_2^{(m)} > \lambda_2^{(m+1)}$ for all m. When $\lambda_1 = \lambda_1^{(0)}$ (most regularized), we compute a sequence of solutions across the λ_2 -values (from large to small values): a solution obtained at $(\lambda_1^{(0)}, \lambda_2^{(m)})$ is used to initialize our CD procedure for the value $(\lambda_1^{(0)}, \lambda_2^{(m+1)})$. As the number of nonzeros in a solution to (7) generally increases with λ_2 -values, our CD procedure for $(\lambda_1^{(0)}, \lambda_2^{(m+1)})$ uses an active set that is slightly larger than the active set $\lambda_1^{(m)}$ corresponding to the solution at $\lambda_1^{(0)}$, $\lambda_2^{(m)}$. Once we have traced a full path over λ_2 , we use warm-starts in the lateral direction across the space of λ_1 . For all $k \geq 0$, to obtain a solution to (7) at $\lambda_1^{(k+1)}, \lambda_2^{(m)}$, we use the solution at $\lambda_1^{(k)}, \lambda_2^{(m)}$ as a warm-start.

4.2 Algorithms for sparse hierarchical interactions: Problem (8)

Similar to the case of (7), and with the computational speed in mind, we present approximate methods to obtain good solutions to (9). As mentioned earlier, these approximate solutions can be used to initialize MIP-based approaches for (9) to improve the solution, and/or to certify the quality of these approximate solutions following Bertsimas et al. [2016], Hazimeh and Mazumder [2020a].

Our first step is to reduce the number of main and interaction effects in (8) by making use of the family of solutions available from (7). We consider the union of supports available from the family of solutions obtained from (7), across the 2D grid of tuning parameters λ_1, λ_2 . Let $\mathcal{M} \subset [p]$ and $\mathcal{I} \subset [p(p-1)/2]$ denote the sets of all nonzero main effects and interactions effects, respectively¹², encountered along the 2D path of solutions to (7). We form a reduced version of problem (9) with $z_i = 0, i \notin \mathcal{M}$ and $z_{j,k} = 0$ for all $(j,k) \notin \mathcal{I}$. Let us denote the reduced problem by $\mathcal{P}(\mathcal{M},\mathcal{I})$. We consider a convex relaxation of $\mathcal{P}(\mathcal{M},\mathcal{I})$, denoted by $\mathcal{P}^R(\mathcal{M},\mathcal{I})$, where all binary variables $\{z_i\}$, $\{z_{j,k}\}$ in $\mathcal{P}(\mathcal{M},\mathcal{I})$ are relaxed to the interval [0,1]. As the sizes of \mathcal{M} and \mathcal{I} are generally small, it is computationally feasible to solve the relaxation $\mathcal{P}^R(\mathcal{M},\mathcal{I})$ – we let $\{z_i^R\}$ and $\{z_{j,k}^R\}$ denote a solution to this relaxation. Following Hazimeh and Mazumder [2020b], it can be shown that this solution satisfies the strong hierarchy constraint (almost surely). To obtain a feasible solution to Problem (9), we apply a relax-and-round procedure. For the rounding step, we consider a threshold $\tau \in (0,1)$ and obtain $\tilde{z}_i = \mathbb{1}[z_i^R > \tau]$ for all $i \in \mathcal{M}$ and $\tilde{z}_{j,k} = \mathbb{1}[z_{j,k}^R > \tau]$ for all $(j,k) \notin \mathcal{I}$. We set $\tilde{z}_i = 0$, $i \notin \mathcal{M}$; and $\tilde{z}_{j,k} = 0$ for all $(j,k) \notin \mathcal{I}$. It can be verified that this rounding procedure maintains strong hierarchy.

¹⁰That is, we check if optimal solutions to (13) and (14) are zero for all blocks outside Q.

¹¹This is usually taken to be 1-10% larger than the current active set, and is chosen in a greedy fashion from among the main and interaction effects lying outside the current active set.

 $^{^{12}}$ If \mathcal{I} includes an interaction (j,k) where main-effect j is not included in \mathcal{M} , we expand \mathcal{M} to include j. This way, we make sure that all interaction effects have the corresponding main effects included in \mathcal{M} .

Finally, we perform a 'polishing' step where we solve (6) restricted to the support defined by $\{\tilde{z}_i\}_i$ and $\{\tilde{z}_{j,k}\}_{j,k}$.

Related Work. In contrast to Problem (7), the regularization penalty in problem (9) is not separable across the blocks due to the overlapping groups created by the strong hierarchy constraint. Hence, the CD-based procedures discussed for (7) do not apply to the hierarchical setting. To the best of our knowledge, there are no prior specialized algorithms for (8) that apply to the scale that we consider here. In fact, even in the linear regression setting, current algorithms for problems with a hierarchy constraint are somewhat limited in terms of the problem-scales they can address. The sole exceptions appear to be the convex optimization based approaches of Lim and Hastie [2015], Hazimeh and Mazumder [2020b], which can address sparse linear regression problems with a large number of features and a small number of observations.

5 Case study: Predicting the Census Survey Self-Response Rate

In this section, we focus on the Census application and present the performance of our approaches in terms of prediction and model parsimony, comparing it to that of existing methods. We also present an interpretation of our results and discuss managerial implications. As we mention in the Introduction, obtaining interpretable models with good predictive capabilities is critically important to practitioners in this application context – such models have the potential to directly influence the planning of outreach campaigns and enable stakeholders to make well-informed decisions on the allocation of spending for different communications channels (for example, TV, radio, digital), advertising messages with properly tailored content, and the timing of spending during the campaigns [Kulzick et al., 2019].

The data we use for this study is publicly available in the US Census Planning Database, which provides a range of demographic, socioeconomic, housing, and Census operational data [US Census Bureau, 2019]. The data in the Planning Database includes covariates from the 2010 Census and the 2013-2017 American Community Survey (ACS), aggregated at both the Census tract level and the block level. We use tract level data, with approximately 74,000 observations and 500 covariates. We take the dependent variable to be the ACS self-response rate. Based on discussions with the stakeholders, for interpretability reasons, we exclude the following covariates from our model: spatial covariates (State, County, Tract, Flag, AIAN Land); and variables that serve as a proxy to our response (for example, Low response score, number of housing units that returned first forms, replacement forms or bilingual forms in Census 2010). We also remove the margin of error variables corresponding to the ACS. After excluding these variables, we are left with p=295 covariates. To clarify, the numerical results that follow are based on p=295 features, though we have tested the scalability of our approach for up to p=500.

5.1 Experimental setup

We randomly split the data into 58K observations for training, 7.2K observations for validation (used for hyperparameter selection), and 7.2K observations for final evaluation (testing). We train all models with the standard squared error loss. In terms of evaluation metrics, we consider root mean square error (RMSE) and mean absolute error (MAE) on the held-out test set (validation is done using the corresponding metric). In addition, we consider variable selection performance – for example, with respect to the number of features retained and the associated interpretations they offer. As noted in Bates and Mulry [2011], the standard current approach for such analysis is based on a linear regression model with \sim 25 hand-selected features. The authors also discuss using tailored variable transformations on some of the features to incorporate nonlinear effects. Such a pursuit would be impractical in our situation, as we have to deal with a large number of features along with

the corresponding pairwise interactions. However, as we use nonparametric models, which seek to learn nonlinearities in the main and interaction effects, such feature engineering may not be necessary.

We apply covariate-wise standardization with training data means and variances, and use the same transformations for the validation and test sets.

Benchmark Methods. We evaluate and compare our models against existing linear and nonparametric approaches. We consider the following linear models with main effects only (i.e., without interactions): (i) Ridge regression; (ii) Lasso regression [Hastie et al., 2015]; (iii) ℓ_0 -penalized regression with additional ridge regularization (denoted as $\ell_0 - \ell_2$), implemented via LOLearn proposed in [Hazimeh and Mazumder, 2020a]. In addition, we consider the following linear models with interaction effects: (iv) Lasso with main effects and all pairwise linear interactions, (v) hierScale: convex estimation framework for learning sparse interactions under a strong hierarchy constraint [Hazimeh and Mazumder, 2020b]. For (i), (ii) and (iv) we use Python's scikit-learn library [Pedregosa et al., 2011]. In addition to the aforementioned linear model benchmarks, we also compare against state-of-the-art black-box machine learning methods such as (vi) XGBoost (gradient Boosting machines) [Chen and Guestrin, 2016]; and (vii) Feedforward neural networks¹³.

Proposed Models. We consider different variants of our proposed approaches, and compare them to the benchmarks above. More specifically, we consider (a) ℓ_0 -penalized Additive Models (AMs) with nonlinear main effects, and the following models containing both the main and the interaction effects: (b) ℓ_0 -penalized AMs with both main and interaction effects, i.e., estimator (7); and (c) sparse hierarchical interactions, i.e., estimator (8). For all our methods, we use 2000 values of the tuning parameters.

All our algorithms for estimators (a)–(c) above are implemented in Python. We use cubic B-splines with 10 knots for the main effects. For the interaction effects we use tensor spline bases of degree 3 with 5 knots in each coordinate, leading to a total of $5 \times 5 = 25$ knots. Because the problem at hand has 295 covariates and 43,365 possible pairwise interactions, we need to be careful with implementation aspects while generating spline-transformed representations for all the interaction effects, which can be memory intensive.

For method (b), i.e., estimator (7), we set $\alpha = 1$, so that both the main and the interaction effects have the same ℓ_0 -penalty parameter. We note, however, that the strong hierarchy constraint in (8) implicitly gives higher priority to the main effects as compared to the interaction effects. For estimator (c), i.e., Problem (8), we fix the smoothing parameter λ_1 to the optimal value available from (b), to reduce tuning. The parameter τ is chosen based on validation tuning.

5.2 Comparing different methods: prediction, sparsity and interpretability

We compare the models in terms of their prediction and variable selection properties.

Additive nonlinear models vs black-box ML methods. Table 1 reports the prediction errors (RMSE and MAE) on the test-set along with the number of nonzero features in the model. Interestingly, we observe that the test performance of AMs with sparse interactions (both with and without the hierarchy constraints) is comparable to that of the best black box predictive ML models (XGBoost, Neural Networks), when one takes into account the model standard errors. In terms of the RMSE values, XGBoost is the winner followed by AMs with ℓ_0 -sparse interactions without hierarchy (7), and then AMs with sparse hierarchical interactions (8). A similar observation holds for the MAE values. Interpretability (model sparsity and/or hierarchy) is the key differentiating factor among the leading

 $^{^{13}}$ We tune both of the non-parametric models (vi) and (vii) with random search procedures using Python package hyperopt [Bergstra et al., 2015] for hyperparameter optimization. XGBoost is tuned with respect to the maximum depth, number of estimators, gamma, learning rate, minimum child weight, and lambda. Neural networks are tuned with respect to the number of dense layers, number of units in dense layers, choice and strength of regularizers (ℓ_1 , ℓ_2 , dropout), learning rates for Adam optimizer [Kingma and Ba, 2015], and batch sizes. The number of tuning parameters for all the nonparametric models is capped at 2000.

Table 1: Comparisons of our methods with several benchmark models as discussed in the text. We display the tuned RMSE and MAE values for the different models, along with the corresponding number of covariates. LMs and AMs that include pairwise interaction effects are denoted by "..+Interactions". The shorthand 16 Mn + 174 Int (for example) refers to 16 main effects and 174 interaction effects in the selected model, this model contains 160 effective features. The best metrics are highlighted in bold. Numbers within parentheses provide the standard errors.

Type	Model	RMSE	MAE	#Covariates
Linear Models (LMs)	Ridge	6.804 (0.080)	5.254 (0.051)	295
	Lasso	6.803 (0.080)	5.254 (0.051)	221
	L0Learn $(\ell_0 - \ell_2)$	6.813 (0.080)	5.268 (0.051)	136
	LM+Interactions (Lasso)	6.528 (0.077)	5.026 (0.049)	264
				(76 Mn + 1598 Int)
	LM+Interactions with	6.621 (0.078)	5.086 (0.049)	276
	Strong Hierarchy (hierScale)			(276 Mn + 4885 Int)
Nonparametric Additive Models (AM)	AM under ℓ_0 (ours)	6.593 (0.078)	5.120 (0.049)	182
	\mathbf{AM} +Interactions under ℓ_0	6.467 (0.077)	4.973 (0.049)	160
	(ours)			(16 Mn + 174 Int)
	AM+Interactions with	6.452 (0.076)	4.995 (0.049)	131
	Strong Hierarchy (ours)			(131 Mn + 173 Int)
Nonparametric	XGBoost	6.440 (0.076)	4.973 (0.049)	295
(Non-interpretable)	Feedforward Neural Networks	6.501 (0.077)	4.996 (0.049)	295

prediction methods. Model (7), i.e., AMs with sparse interactions, selects fewer main effects and interaction effects (16Mn + 174Int) when compared to AMs with hierarchical interactions (131Mn+173Int), however, the former model does not obey the hierarchy constraint. On the other hand, model (8), i.e., AMs with sparse interactions and hierarchy, selects fewer effective features than (7), which is important in terms of cost-savings from an operational standpoint.

In contrast, the black-box ML methods offer limited interpretability when compared to the AMs proposed here (additional discussions are provided further below). While Table 1 presents a summary of the best models chosen based on the validation set prediction performance, one can also consider alternatives if the stakeholders have a preference for obtaining models with fewer features (perhaps at the cost of a marginal deterioration in predictive performance) – see Section 5.3 for further discussion.

Nonlinear models vs linear models. Table 1 shows that nonlinear models have significantly better predictive performance than their linear counterparts; and linear models with sparse interactions appear to have the edge over linear models without interactions. Another appealing aspect of AMs with nonlinear components lies in model parsimony (we alluded to this aspect in Figure 2 with a reduced number of features). We observe that the number of nonzero main and interaction effects is significantly lower for the nonlinear additive models. For example, AMs under ℓ_0 can achieve the same level of predictive performance as LoLearn with significantly fewer covariates: 40 versus 136. Similarly, if we compare hierScale to the proposed AMs with interactions under strong hierarchy, the number of main effects reduces from 276 to 131, and the number of interaction effects reduces from 4,885 to 173.

Additive nonlinear models: interactions vs no interactions. For AMs under ℓ_0 , we can reduce the number of effective covariates, from 182 to 131, by including the interaction effects. This could be due to the fact that a large number of nonlinear main effects attempt to explain the nonlinear interaction effects. The resulting compression highlights the redundancy of some of the covariates when interaction effects are directly included in the model. Furthermore, the prediction performance of nonlinear AMs seems to improve when the interactions are taken into account.

Partial dependence association plots. Building off of Figure 1, which illustrates some marginal nonlinear fits, an appealing aspect of AMs is that they naturally allow the practitioner to gather insights from the marginal association between y and x_j by making use of the map $x_j \mapsto f_j(x_j)$ and, similarly, from the interaction effect y versus (x_j, x_k) via the learned map $(x_j, x_k) \mapsto f_{j,k}(x_j, x_k)$. This is a by-product of the additive model – such interpretations, however, are not readily available via black-box ML methods such as Neural Networks and XGBoost.

Marginal fits can, for example, help the stakeholders identify promising factors potentially leading to the largest benefits in terms of maximizing the actual self-response score – these insights can in turn impact policy decisions regarding targeted investments and optimizing the operational costs.

In summary, our proposed framework – AMs with sparse nonlinear main and interaction effects – allows for automated variable selection, provides simple interpretability, and delivers useful insights into the underlying marginal associations/relationships between the covariates and the response. Given their strong predictive performance relative to the black-box ML methods, our proposed approach has the potential to be highly useful in the context of the US Census application that originally motivated this study.

Insights from visualizations. To obtain a finer understanding of the performance of our models, we use some visualization tools inspired by US Census Bureau [2017], Kulzick et al. [2019].

Figure 3 visualizes the tract self-response rates predicted by our proposed AMs with interactions approach on a map of the United States. The North in general, and the Upper Midwest and the Northeast in particular, have higher self-response rates than the rest of the country. Tracts with lower self-response rates are visible in many states – in particular, in the South and in the Mountain region of the United States.

Figure 4 displays, side by side, the actual and the predicted self-response rates for the tracts in Washington DC, as well as the corresponding differences. Both the actual and the predicted rates are higher than average in most parts of the Northwest and a portion of the Northeast DC, and lower in the Southeast and most of the Northeast DC. A visualization of the self-response rates predicted by our proposed AMs with interactions approach, for all the tracts in the US, is provided in the Supplement.

Figure 5 shows how the sorting of the Census tracts into quintiles of the actual self-response rates

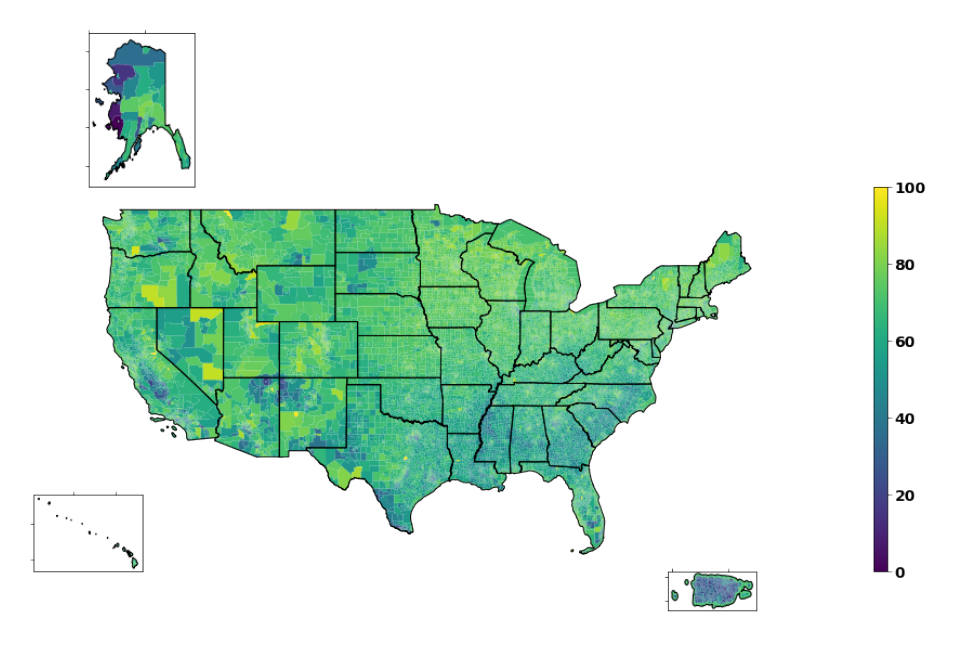


Figure 3: Predicted ACS self-response rates for all tracts in the United States.

18

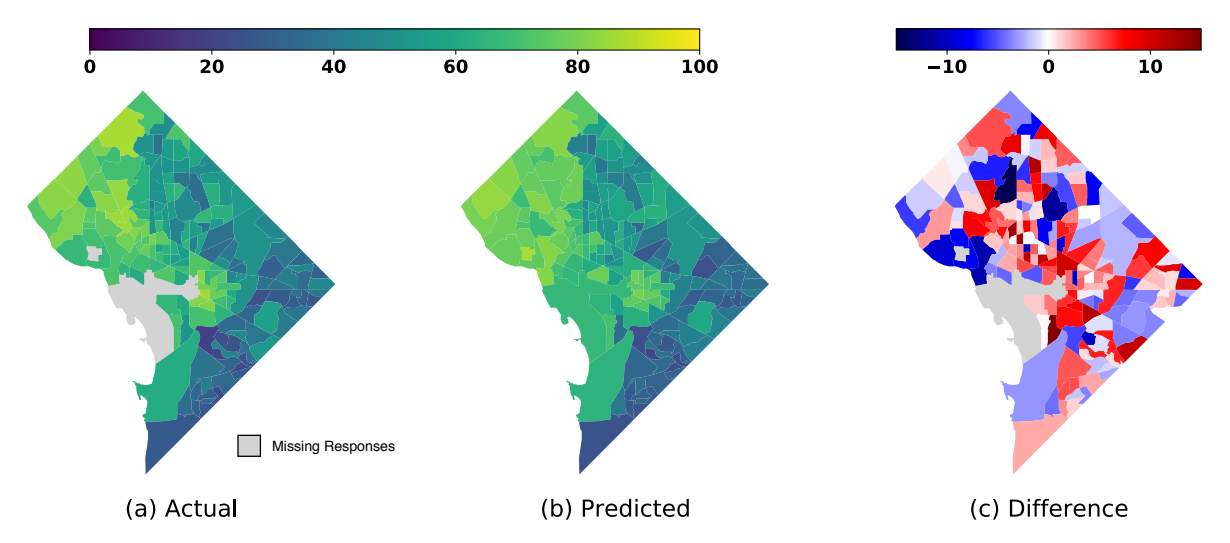


Figure 4: ACS self-response rates for all tracts in the District of Columbia. a) Actual ACS self-response rates. b) Predicted ACS self-response rates for AMs with interactions (7). c) Difference between the actual and predicted self-response rate: difference = actual - predicted.

compares with the corresponding sorting of the predictions made by either AMs with interactions (7) or the Lasso (we use an ℓ_1 -penalized linear model with main effects and no interactions). For example, the top panel in Figure 5 shows that among the tracts in the first quintile of the actual self-response rates,

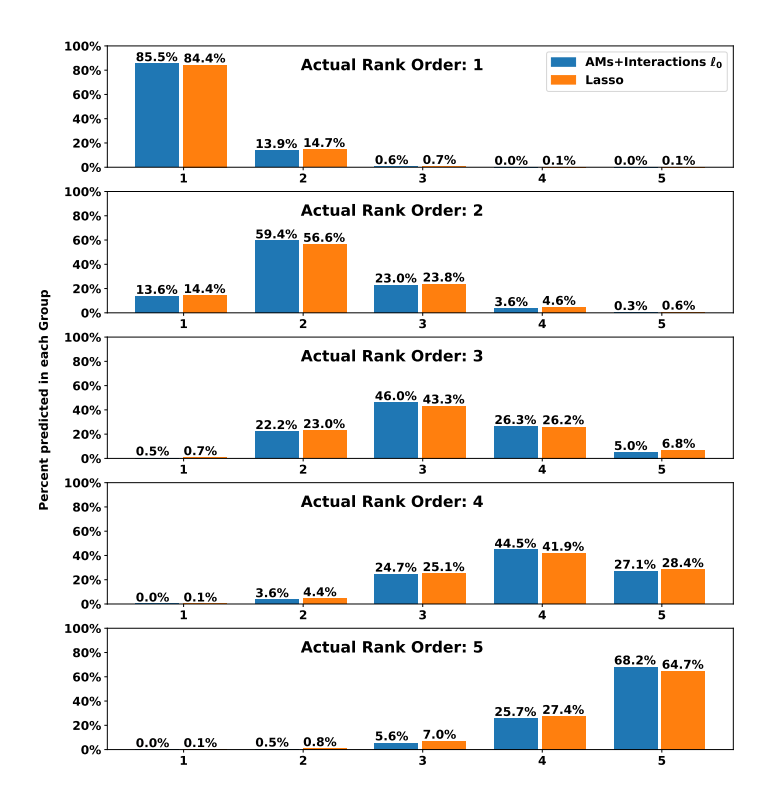


Figure 5: Comparison of quintile groups based on Lasso regression (linear model with main effects) US Census Bureau [2017], Kulzick et al. [2019] and our proposed AM with main-effects and interactions under ℓ_0 sparsity.

•

85.3% are correctly predicted by AMs with interactions to fall in the first quintile; the corresponding proportion for the Lasso is 84.4%. The same panel shows that among the tracts in the first quintile of the actual self-response rates, 13.8% are incorrectly predicted to fall in the second quintile; this proportion is smaller than the one for the Lasso (14.7%). Similarly, in the second quintile of the actual self-response rates, a higher proportion (59.4%) is correctly identified by our AMs with interactions to be in the second quintile; this is again an improvement over the 56.6% for the Lasso regression model. For all 5 quintiles (rank orders 1-5) of the actual self response rates, AMs with interactions identify a higher proportion to be in the correct quintile than the Lasso. Overall, Figure 5 suggests that AMs with interactions perform better than the Lasso.

5.3 Interpreting important features

We illustrate how our methodology can guide us to obtain a set of interpretable features and derive associated actionable insights into the factors contributing towards low response-rates in surveys. An important aspect of our framework is that it provides an automated scheme to identify a collection of models, balancing out the complexity of the model and the data-fidelity (or prediction accuracy). For example, Figure 6[left panel] plots the number of main and interaction effects versus the associated prediction error for model (7). The plot illustrates that by trading off a little in the predictive performance (in terms of RMSE, which is shown by the red dashed line), we can limit the number of effects at any level, as desired by the practitioner, who intends to obtain a more granular understanding of the factors impacting the survey response rates.

Specifically, if we would like to limit the number of main effects to under 20, Figure 6(b) shows the top 19 main effects in the order they enter the model along the regularization path. The definitions of the variables in Figure 6(b) are provided in the Supplement. Most of these variables also appear in the selected models reported in Erdman and Bates [2016] and Kulzick et al. [2019], and some can be interpreted in the context of clusters defined in Bates and Mulry [2011] or mindset solutions in Kulzick et al. [2019].

Using cluster analysis, Bates and Mulry [2011] categorize the covariates in a self-response prediction model into eight distinct clusters: All Around Average I (Homeowner Skewed), All Around Average II (Renter Skewed), Economically Disadvantaged I (Homeowner Skewed), Economically Disadvantaged II (Renter Skewed), Ethnic Enclave I (Homeowner Skewed), Ethnic Enclave II (Renter Skewed), Single

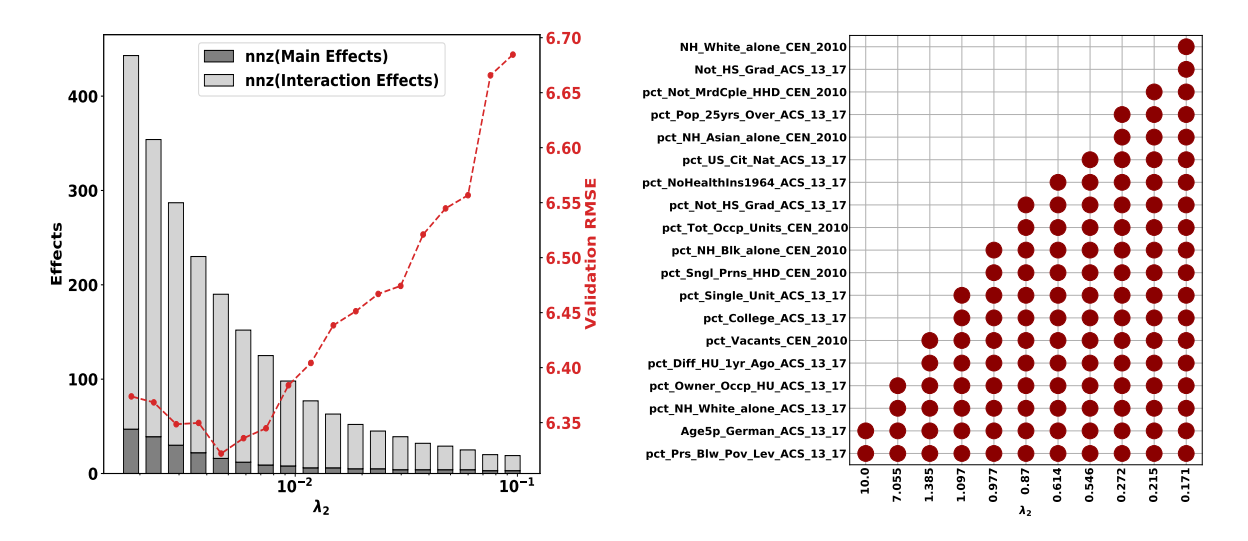


Figure 6: Properties of model (7), AMs with interactions. [Left] # nonzero effects vs the corresponding RMSE. [Right] Variables corresponding to main effects selected by the model as the regularization penalty is varied: for visualization purposes, we focus on the top 19 main effects.

Unattached Mobiles, and Advantaged Homeowners. From the description of these clusters in Bates and Mulry [2011], we see that the variables listed in Figure 6[right panel] that are related to poverty and no health insurance belong to the Economically Disadvantaged clusters. On the other hand, variables related to ethnic groups and/or English language proficiency belong to the Ethnic Enclave clusters.

Some of the covariates in Figure 6[right] can also be interpreted in terms of the mindset solutions in Kulzick et al. [2019]. In a mindset solution, survey respondents are categorized using factor analysis into six mindsets based on their predicted self-response patterns and demographic characteristics. These mindsets are determined by the demographic characteristics such as age, race, income, home-ownership, presence of children in the household, marital status, internet use, English proficiency, and country of birth. The six mindsets are: Eager Engagers, Fence Sitters, Individuals with a Confidentiality, Head Nodders, Wary Skeptics and Disconnected Doubters. The covariates can be also interpreted in terms of eight segmented tracts: Responsive Suburbia, Main Street Middle, Country Roads, Downtown Dynamic, Student and Military Communities, Sparse Spaces, Multicultural Mosaic, and Rural Delta and Urban Enclaves – see Kulzick et al. [2019] for additional details.

6 Conclusion

Low-response rates in surveys and censuses remain a continual source of concern. We present new interpretable statistical methods to accurately predict response rates in surveys based on the US Census Planning Database. We use a nonparametric additive model with nonlinear main effects and pairwise interactions for the conditional mean of the output. We employ ℓ_0 -penalization to promote sparsity in the components, and also allow for structured variants to promote variable selection under a strong hierarchy constraint – to our knowledge, this is the first time such approaches are being studied in the context of nonparametric additive models with pairwise interactions. We also present novel statistical guarantees for our estimators, establishing non-asymptotic error bounds that allow for model misspecification and apply to the high-dimensional setting. Despite their appeal and strong methodological underpinnings, the proposed models lead to computational challenges. To this end, we present, to the best of our knowledge, the first scalable algorithms for structured feature selection within these nonparametric models, which scale to instances with $n \approx 10^5$ observations and $p \approx 500$ features, with $p^2 \approx 10^5$ interactions.

Empirically, we observe that our proposed approach leads to strong predictive performance while simultaneously delivering a parsimonious and interpretable model. The prediction performance of our highly interpretable models matches the performance of the best predictive models produced by black-box ML methods such as XGBoost and Neural Networks.

From a practical standpoint, our goal has been to create a framework to help practitioners identify key factors that influence survey response rates. Insights gathered from our statistical models may be used for targeted follow-up surveys and allocation of resources for advertisements, among others. We hope that such models will facilitate the goal of having a census that is cost effective and results in improved coverage in a timely and accurate fashion, while optimizing the operational risks and costs. Our framework can be potentially used to complement the LRS metric that is currently used in the US Census Bureau ROAM application.

Although in this paper we consider a particular Census application, our methodology is general and may be of interest in other applied settings as well.

Acknowledgements

The authors would like to thank Nancy Bates, Tommy Wright and Joanna Fane Lineback from the U.S. Census Bureau for helpful discussions. Thanks also to other researchers from the Centers for Statistical Research and Methodology and Behavioral Science Methods (U.S Census Bureau) for helpful feedback in earlier versions of this work. Any opinions and conclusions expressed herein are those of the authors and do not necessarily represent the views of the U.S. Census Bureau. This research was supported

in part, by grants from the Office of Naval Research: ONR-N000141812298 (YIP) and the National Science Foundation: NSF-IIS-1718258 awarded to Rahul Mazumder.

References

- Chandra Erdman and Nancy Bates. The low response score (LRS). *Public Opinion Quarterly*, 81(1): 144–156, December 2016. doi: 10.1093/poq/nfw040.
- Tom W. Smith. Hard-to-survey populations in comparative perspective. In Roger Tourangeau, Brad Edwards, Timothy P. Johnson, Kirk M. Wolter, and Nancy Bates, editors, *Hard-to-Survey Populations*, pages 21–36. Cambridge University Press, Cambridge, 2014. ISBN 9781139381635. doi: 10.1017/CBO9781139381635.004.
- Roger Tourangeau, Brad Edwards, Timothy P Johnson, Kirk M Wolter, and Nancy Bates. *Hard-to-survey populations*. Cambridge University Press, 2014.
- US Census Bureau. 2010 census integrated communications campaign plan: The success of the census is in our hands. November 2009.
- Nancy Bates and Mary H. Mulry. Using a geographic segmentation to understand, predict, and plan for census and survey mail nonresponse. *Journal of Official Statistics*, 27(4):601–618, July 2011.
- Tom Mule. 2010 census coverage measurement estimation report: Summary of estimates of coverage for persons in the united states. Dssd 2010 census coverage measurement memorandum series no. 2010-g-01, US Census Bureau, May 2012.
- Antonio Bruce, J Gregory Robinson, and Monique V Sanders. Hard-to-count scores and broad demographic groups associated with patterns of response rates in census 2000. In *Joint Statistical Meeting*, 2001.
- Trevor Hastie and Robert Tibshirani. Generalized additive models: some applications. *Journal of the American Statistical Association*, 82(398):371–386, 1987.
- Trevor Hastie, Robert Tibshirani, and Jerome Friedman. *The Elements of Statistical Learning*. Springer Series in Statistics. Springer New York Inc., New York, NY, USA, 2001.
- Francis Bach, Rodolphe Jenatton, Julien Mairal, and Guillaume Obozinski. Structured sparsity through convex optimization. *Statistical Science*, 27(4):450–468, November 2012. doi: 10.1214/12-sts394.
- Dimitris Bertsimas, Angela King, and Rahul Mazumder. Best subset selection via a modern optimization lens. *Annals of Statistics*, 44(2):813–852, 2016.
- Rahul Mazumder and Peter Radchenko. The Discrete Dantzig Selector: Estimating sparse linear models via mixed integer linear optimization. *IEEE Transactions on Information Theory*, 63 (5): 3053 3075, 2017.
- Rahul Mazumder, Peter Radchenko, and Antoine Dedieu. Subset selection with shrinkage: Sparse linear modeling when the snr is low. arXiv preprint arXiv:1708.03288, 2017.
- Hussein Hazimeh and Rahul Mazumder. Fast best subset selection: Coordinate descent and local combinatorial optimization algorithms. *Oper. Res.*, 68(5):1517–1537, September 2020a. ISSN 0030-364X. doi: 10.1287/opre.2019.1919.

- Hussein Hazimeh and Rahul Mazumder. Learning hierarchical interactions at scale: A convex optimization approach. In Silvia Chiappa and Roberto Calandra, editors, *Proceedings of the Twenty Third International Conference on Artificial Intelligence and Statistics*, volume 108 of *Proceedings of Machine Learning Research*, pages 1833–1843. PMLR, 26–28 Aug 2020b.
- Jacob Bien, Jonathan Taylor, and Robert Tibshirani. A lasso for hierarchical interactions. *The Annals of Statistics*, 41(3):1111–1141, June 2013. doi: 10.1214/13-aos1096.
- Laurence A Wolsey and George L Nemhauser. *Integer and combinatorial optimization*, volume 55. John Wiley & Sons, 1999.
- Yurii Nesterov. Introductory lectures on convex optimization: A basic course, volume 87. Springer Science & Business Media, 2003.
- Lukas Meier, Sara van de Geer, and Peter BÃCEhlmann. High-dimensional additive modeling. *The Annals of Statistics*, 37(6B):3779 3821, 2009. doi: 10.1214/09-AOS692.
- Pradeep Ravikumar, John Lafferty, Han Liu, and Larry Wasserman. Sparse additive models. *Journal of the Royal Statistical Society: Series B (Statistical Methodology)*, 71(5):1009–1030, November 2009. doi: 10.1111/j.1467-9868.2009.00718.x.
- J. Huang, J.L. Horowitz, and F. Wei. Variable selection in nonparametric additive models. The Annals of Statistics, 38:2282–2313, 2010.
- Vladimir Koltchinskii and Ming Yuan. Sparsity in multiple kernel learning. *The Annals of Statistics*, 38(6):3660–3695, 2010.
- Tuo Zhao and Han Liu. Sparse additive machine. In Neil D. Lawrence and Mark Girolami, editors, Proceedings of the Fifteenth International Conference on Artificial Intelligence and Statistics, volume 22 of Proceedings of Machine Learning Research, pages 1435–1443, La Palma, Canary Islands, 21–23 Apr 2012. PMLR.
- Ming Yuan and Ding-Xuan Zhou. Minimax optimal rates of estimation in high dimensional additive models. *The Annals of Statistics*, 44(6):2564–2593, 2016.
- Hussein Hazimeh, Rahul Mazumder, and Peter Radchenko. Grouped variable selection with discrete optimization: Computational and statistical perspectives. arXiv preprint arXiv:2104.07084, 2021.
- Grace Wahba. Spline Models for Observational Data. Society for Industrial and Applied Mathematics, January 1990. doi: 10.1137/1.9781611970128.
- Charles J Stone. The dimensionality reduction principle for generalized additive models. *The Annals of Statistics*, pages 590–606, 1986.
- Trevor Hastie, Robert Tibshirani, and Martin Wainwright. Statistical Learning with Sparsity: The Lasso and Generalizations. Chapman & Hall/CRC, 2015. ISBN 1498712169, 9781498712163.
- Peter Radchenko and Gareth M. James. Variable selection using adaptive nonlinear interaction structures in high dimensions. *Journal of the American Statistical Association*, 105(492):1541–1553, December 2010. doi: 10.1198/jasa.2010.tm10130.
- Peter Hall and J. D. Opsomer. Theory for penalised spline regression. *Biometrika*, 92(1):105–118, March 2005. doi: 10.1093/biomet/92.1.105.
- Yingxing Li and David Ruppert. On the asymptotics of penalized splines. *Biometrika*, 95(2):415–436, 2008. ISSN 00063444.

- Simon N. Wood. Low-rank scale-invariant tensor product smooths for generalized additive mixed models. *Biometrics*, 62(4):1025–1036, May 2006. doi: 10.1111/j.1541-0420.2006.00574.x.
- Paul H. C. Eilers and Brian D. Marx. Flexible smoothing with b-splines and penalties. *Statistical Science*, 11:89–121, 1996.
- E. E. Kammann and M. P. Wand. Geoadditive models. *Journal of the Royal Statistical Society: Series C (Applied Statistics)*, 52(1):1–18, January 2003. doi: 10.1111/1467-9876.00385.
- Paul H.C. Eilers and Brian D. Marx. Multivariate calibration with temperature interaction using two-dimensional penalized signal regression. *Chemometrics and Intelligent Laboratory Systems*, 66 (2):159–174, June 2003. doi: 10.1016/s0169-7439(03)00029-7.
- C. Erdman and Nancy J. Bates. The u.s. census bureau mail return rate challenge: Crowdsourcing to develop a hard-to-count score. 2014.
- US Census Bureau. Planning database, Jun 2019.
- Hussein Hazimeh, Rahul Mazumder, and Ali Saab. Sparse regression at scale: Branch-and-bound rooted in first-order optimization. arXiv preprint arXiv:2004.06152, 2020.
- Peter Buhlmann and Sara van de Geer. Statistics for High-Dimensional Data: Methods, Theory and Applications. Springer Publishing Company, Incorporated, 1st edition, 2011. ISBN 3642201911.
- Peter McCullagh and John A Nelder. Generalized linear models, volume 37. CRC press, 1989.
- Michael Lim and Trevor Hastie. Learning interactions via hierarchical group-lasso regularization. Journal of Computational and Graphical Statistics, 24(3):627–654, July 2015. doi: 10.1080/10618600. 2014.938812.
- Xiaohan Yan and Jacob Bien. Hierarchical sparse modeling: A choice of two group lasso formulations. *Statistical Science*, 32(4):531–560, November 2017. doi: 10.1214/17-sts622.
- Zhiqiang Tan and Cun-Hui Zhang. Doubly penalized estimation in additive regression with high-dimensional data. *The Annals of Statistics*, 47(5):2567–2600, 2019.
- K. Lounici, M. Pontil, S. van de Geer, and A. Tsybakov. Oracle inequalities and optimal inference under group sparsity. *The Annals of Statistics*, 39(4):2164–2204, 2011.
- Y. Lin and H. H. Zhang. Component selection and smoothing in multivariate nonparametric regression. *The Annals of Statistics*, 34:2272–2297, 2006.
- Simon N. Wood, Zheyuan Li, Gavin Shaddick, and Nicole H. Augustin. Generalized additive models for gigadata: Modeling the u.k. black smoke network daily data. *Journal of the American Statistical Association*, 112(519):1199–1210, April 2017. doi: 10.1080/01621459.2016.1195744.
- Stephen J Wright. Coordinate descent algorithms. Mathematical Programming, 151(1):3–34, 2015.
- Jerome Friedman, Trevor Hastie, and Robert Tibshirani. Regularization paths for generalized linear models via coordinate descent. *Journal of Statistical Software*, 33(1), 2010. doi: 10.18637/jss.v033. i01.
- Robert Kulzick, Laura Kail, Shawnna Mullenax, Hubert Shang, Brian Kriz, Gina Walejko, Monica Vines, Nancy Batesand Steven Scheid, , and Yazmín García Trejo. 2020 census predictive models and audience segmentation report. June 2019.

- Fabian Pedregosa, Gaël Varoquaux, Alexandre Gramfort, Vincent Michel, Bertrand Thirion, Olivier Grisel, Mathieu Blondel, Peter Prettenhofer, Ron Weiss, Vincent Dubourg, Jake Vanderplas, Alexandre Passos, David Cournapeau, Matthieu Brucher, Matthieu Perrot, and Édouard Duchesnay. Scikitlearn: Machine learning in python. *J. Mach. Learn. Res.*, 12(null):2825–2830, November 2011. ISSN 1532-4435.
- Tianqi Chen and Carlos Guestrin. XGBoost: A scalable tree boosting system. In *Proceedings of the 22nd ACM SIGKDD International Conference on Knowledge Discovery and Data Mining*, KDD '16, pages 785–794, New York, NY, USA, 2016. ACM. ISBN 978-1-4503-4232-2. doi: 10.1145/2939672. 2939785.
- James Bergstra, Brent Komer, Chris Eliasmith, Dan Yamins, and David D Cox. Hyperopt: a python library for model selection and hyperparameter optimization. *Computational Science & Discovery*, 8(1):014008, 2015.
- Diederik P. Kingma and Jimmy Ba. Adam: A method for stochastic optimization. In Yoshua Bengio and Yann LeCun, editors, 3rd International Conference on Learning Representations, ICLR 2015, San Diego, CA, USA, May 7-9, 2015, Conference Track Proceedings, 2015.
- US Census Bureau. Foundational communications models 1.0: the updated low response score (lrs) and an internet lrs. 2017.
- John Tinsley Oden and Junuthula Narasimha Reddy. An introduction to the mathematical theory of finite elements. Wiley, New York, 1976.
- Sara Van de Geer. Empirical Processes in M-Estimation. Cambridge University Press, Cambridge, 2000.
- S Agmon. Lectures on Elliptic Boundary Value Problems. Van Nostrand, Princeton, NJ, 1965.
- M. S. Birman and M. Z. Solomjak. Piecewise-polynomial approximations of functions of the classes w_p^{α} . *Math. USSR-Sbornik*, 2(3):295–317, 1967.

Supplementary Material

This supplemental document contains some additional results not included in the main body of the paper. In particular, we present

- proofs for Theorem 1 in Section 3.
- Census variable descriptions for Figure 2 in Section 2.2 and Figure 6b in Section 5.3.

This supplement is not entirely self-contained, so readers might need to refer to the main paper.

Contents

S1	Statistics Theory: Proofs	27
	S1.1 Preliminaries and supplementary results	27
	S1.2 Proof of Theorem 1	28
	S1.3 Proof of Corollary 1	28
	S1.4 Proof of Lemma 1	29
	S1.5 Proof of Lemma 2	30
	S1.6 Proof of Lemma 3	30
S2	2 Definition of important Census/American Community Survey variables	30
	S2.1 Definition of the variables in Figure 2	
	S2.2 Definition of the variables in Figure 6(b)	32
	0 \ /	

S1Statistics Theory: Proofs

S1.1Preliminaries and supplementary results

We will prove a slightly more general result by replacing the 2-nd derivative in the definition of C_{gr} and Ω_{gr} with an m-th derivative, and redefining r_n as $n^{-m/(2m+2)}$. Theorem 1 will then follow as a special case corresponding to m=2.

We extend the domain of $\|\cdot\|_n$ from vectors in \mathbb{R}^n to real-valued functions on $[0,1]^p$ by letting $\|\cdot\|_n$ be the empirical L_2 -norm. Thus, given a function h, we let $\|h\|_n = \left[\sum_{i=1}^n h(\mathbf{x}_i)^2/n\right]^{1/2}$. This extension is consistent in the sense that $||f||_n = ||\mathbf{f}||_n$ for $f \in \mathcal{C}_{gr}$. By analogy with the $||\cdot||_n$ notation, we define $(\epsilon, \mathbf{v})_n = (1/n) \sum_{i=1}^n \epsilon_i v_i$ for each $\mathbf{v} \in \mathbb{R}^n$. For the simplicity of the presentation, we use the double-index notation f_{jj} for the main effect components f_j of functions $f \in \mathcal{C}_{gr}$ and then take advantage of the additive representation

$$\sum_{j \in [p]} f_j(x_j) + \sum_{j < k} f_{j,k}(x_j, x_k) = \sum_{j \le k} f_{j,k}(x_j, x_k).$$

We also define $\tilde{\Omega}(f_{j,k}) = \sqrt{\Omega(f_{j,k})}$ and $\tilde{\Omega}_{gr}(f) = \sum_{j \leq k} \sqrt{\Omega(f_{j,k})}$. We let $\mathcal{J} = \{(j,k) \in [p] \times [p], \text{ s.t. } j \leq k\}$. Given $J \subseteq \mathcal{J}$, we define functional classes $\mathcal{F}(J) = \{f : f(\mathbf{x}) = \sum_{(j,k) \in J} f_{j,k}(x_j,x_k), f_{j,k} \in \mathcal{C}_2\}$ and $\mathcal{H}(J) = \{h : h \in \mathcal{F}(J), \|h\|_n/(r_n + \tilde{\Omega}_{gr}(h) \leq 1\}$; we also let $\mathcal{F}_s = \{f: f \in \mathcal{C}_{gr}, G(f) \leq s\}$ for every natural s. Given a positive constant δ and a metric space \mathcal{H} endowed with the norm $\|\cdot\|$, we use the standard notation and write $H(\delta,\mathcal{H},\|\cdot\|)$ for the δ -entropy of \mathcal{H} with respect to $\|\cdot\|$. More specifically, $H(\delta,\mathcal{H},\|\cdot\|)$ is the natural logarithm of the smallest number of balls with radius δ needed to cover \mathcal{H} . The following result, proved in Section S1.4, bounds the entropy of $\mathcal{H}(J)$.

Lemma 1. $H(u, \mathcal{H}(J), \|\cdot\|_n) \lesssim (1/u)^{2/m}$ for $u \in (0, 1)$.

Let M = K(K+1)/2. We will need the following maximal inequalities, which are proved in Sections S1.5 and S1.6, respectively.

Lemma 2. Suppose that $J \subseteq \mathcal{J}$ and $|J| \leq M$. Then, with probability at least $1 - e^{-t}$, inequality

$$(\epsilon/\sigma, \mathbf{f})_n \lesssim \left[r_n + \sqrt{t/n}\right] \|\mathbf{f}\|_n + \left[r_n^2 + r_n \sqrt{t/n}\right] \tilde{\Omega}_{gr}(f)$$

holds uniformly over $f \in \mathcal{F}(J)$.

Lemma 3. With probability at least $1 - \epsilon$, inequality

$$(\epsilon/\sigma, \mathbf{f})_n \lesssim \left[r_n + \sqrt{\frac{\log(ep)}{n}} + \sqrt{\frac{\log(1/\epsilon)}{n}}\right] \|\mathbf{f}\|_n + \left[r_n^2 + r_n\sqrt{\frac{\log(ep)}{n}} + r_n\sqrt{\frac{\log(1/\epsilon)}{n}}\right] \tilde{\Omega}_{gr}(f)$$

holds uniformly over $f \in \mathcal{F}_M$.

S1.2 Proof of Theorem 1

Consider an arbitrary function $f \in \mathcal{C}_{gr}$. For the remainder of the proof, all universal constants will be chosen independently of f. Because f is feasible for optimization problem (10), we have the following inequality:

$$\|\widehat{\mathbf{f}} - \mathbf{f}^*\|_n^2 + \lambda_n \Omega_{gr}(\widehat{f}) + \mu_n G(\widehat{f}) \le \|\mathbf{f} - \mathbf{f}^*\|_n^2 + 2(\epsilon, \widehat{\mathbf{f}} - \mathbf{f})_n + \lambda_n \Omega_{gr}(f) + \mu_n G(f).$$
 (S1)

Applying Lemma 3 with $f = \hat{f} - f$ and $\epsilon = (ep)^{-1}$, we derive that, with probability at least 1 - 1/p,

$$(\boldsymbol{\epsilon}/\sigma, \widehat{\mathbf{f}} - \mathbf{f})_n \leq c_1 \left[r_n + \sqrt{\frac{\log(ep)}{n}} \right] \|\widehat{\mathbf{f}} - \mathbf{f}\|_n$$

$$+ a_2 \left[r_n^2 + r_n \sqrt{\frac{\log(ep)}{n}} \right] \widetilde{\Omega}_{gr} (\widehat{f} - f)$$
(S2)

for some universal constants a_1 and a_2 . For the remainder of the proof we restrict our attention to the random event on which (S2) holds. Multiplying inequality (S1) by two, using (S2), and letting

$$\tau_n := 2c_1\sigma\Big[r_n + \sqrt{\frac{\log(ep)}{n}}\Big], \ \tilde{\lambda}_n := 4a_2\sigma\Big[r_n^2 + r_n\sqrt{\frac{\log(ep)}{n}}\Big], \ \text{and} \ \lambda_n \geq \tilde{\lambda}_n,$$

we derive

$$2\|\widehat{\mathbf{f}} - \mathbf{f}^*\|_n^2 + 2\lambda_n\Omega_{\mathrm{gr}}(\widehat{f}) + 2\mu_nG(\widehat{f}) \leq 2\|\mathbf{f} - \mathbf{f}^*\|_n^2 + 2\tau_n\|\widehat{\mathbf{f}} - \mathbf{f}\|_n + \tilde{\lambda}_n\tilde{\Omega}_{\mathrm{gr}}(\widehat{f} - f) + 2\lambda_n\Omega_{\mathrm{gr}}(f) + 2\mu_nG(f).$$

Applying inequalities $2\tau_n\|\widehat{\mathbf{f}} - \mathbf{f}^*\|_n \le \tau_n^2 + \|\widehat{\mathbf{f}} - \mathbf{f}^*\|_n^2$ and $2\tau_n\|\mathbf{f}^* - \mathbf{f}\|_n \le \tau_n^2 + \|\mathbf{f} - \mathbf{f}^*\|_n^2$, we arrive at

$$2\|\widehat{\mathbf{f}} - \mathbf{f}^*\|_n^2 + 2\lambda_n \Omega_{gr}(\widehat{f}) + 2\mu_n G(\widehat{f}) \leq \|\widehat{\mathbf{f}} - \mathbf{f}^*\|_n^2 + 3\|\mathbf{f} - \mathbf{f}^*\|_n^2 + 2\tau_n^2$$

$$+\tilde{\lambda}_n \left[\tilde{\Omega}_{gr}(\hat{f}) + \tilde{\Omega}_{gr}(f)\right] + 2\lambda_n \Omega_{gr}(f) + 2\mu_n G(f).$$

Taking into account inequality $\tilde{\Omega}_{\rm gr}(\tilde{f}) \lesssim G(\tilde{f}) + \Omega_{\rm gr}(\tilde{f})$, which holds for any $\tilde{f} \in \mathcal{C}_{\rm gr}$, we conclude that

$$\|\widehat{\mathbf{f}} - \mathbf{f}^*\|_n^2 + \lambda_n \Omega_{gr}(\widehat{f}) + 2\mu_n G(\widehat{f}) \le 3\|\mathbf{f} - \mathbf{f}^*\|_n^2 + a_3 \tau_n^2 + 2\lambda_n \Omega_{gr}(f) + 2\mu_n G(f)$$
(S3)

for some universal constant a_3 .

S1.3 Proof of Corollary 1

The stated prediction error bound is a direct consequence of the bound in Theorem 1, hence we only need to establish the sparsity bound. Taking $f = f^*$, we rewrite inequality (S3) as follows:

$$\|\widehat{\mathbf{f}} - \mathbf{f}^*\|_n^2 + \lambda_n \Omega_{gr}(\widehat{f}) + 2\mu_n G(\widehat{f}) \le a_3 \tau_n^2 + 2\lambda_n \Omega_{gr}(f^*) + 2\mu_n G(f^*).$$
 (S4)

Provided that constant c_2 in the lower bound for μ_n is sufficiently large, we then have $G(\widehat{f}) - G(f^*) < 1$, which implies $G(\widehat{f}) \leq G(f^*)$.

We now focus on the classical asymptotic setting, where p is fixed and n tends to infinity, under the conditions of Corollary 1. Noting that $1/n = o(r_n^2)$ and repeating the arguments in the proofs of Theorem 1 and Corollary 1 with $\epsilon = \exp(-nr_n^2)$, we conclude that inequality (S4) and the accompanying sparsity bound $G(\hat{f}) \leq G(f^*)$ hold with probability tending to one. Imposing an additional requirement that $\lambda_n = O(r_n^2 + \log(ep)/n)$ and $\mu_n = O(r_n^2 + \log(ep)/n)$ then leads to $\|\hat{\mathbf{f}} - \mathbf{f}^*\|_n^2 = O(r_n^2 + \log(ep)/n)$.

S1.4 Proof of Lemma 1

We will establish the stated entropy bound for a somewhat larger functional space $\mathcal{H}'_J = \{h : h \in \mathcal{F}(J), \|h\|_n + \tilde{\Omega}_{gr}(h) \leq 1\}$. We treat m as a fixed universal constant in all inequalities that follow.

Consider an arbitrary $g \in \mathcal{C}_2$. By the Sobolev embedding theorem [for example, Oden and Reddy, 1976, Theorem 3.13], we can write g as a sum of a polynomial of degree m-1 and a function \tilde{g} that satisfies $\|\tilde{g}\|_{L_2} \lesssim \tilde{\Omega}(g)$, where we note that $\tilde{\Omega}(g) = \tilde{\Omega}(\tilde{g})$. Applying Lemma 10.9 in Van de Geer [2000], which builds on the interpolation inequality of Agmon [1965], we derive $\|\tilde{g}\|_{\infty} \lesssim \tilde{\Omega}(\tilde{g})$. Thus, $\mathcal{H}'_J \subseteq \{p + \tilde{h}: p \in \mathcal{P}_J, \ \tilde{h} \in \tilde{\mathcal{H}}_J\}$, where

$$\mathcal{P}_{J} = \{ p : p(\mathbf{x}) = \sum_{(j,k)\in J} \sum_{l=0}^{m-1} \sum_{q=0}^{m-1} \alpha_{j,k,l,q} x_{j}^{l} x_{k}^{q}, \ \alpha_{j,k,l,q} \in \mathbb{R}, \ \|p\|_{n} \le 2 \}$$

$$\tilde{\mathcal{H}}_{J} = \{ \tilde{h} : \tilde{h} \in \mathcal{F}(J), \ \tilde{\Omega}_{gr}(\tilde{h}) \le 1, \ \|\tilde{h}_{j,k}\|_{\infty} \lesssim \tilde{\Omega}(\tilde{h}_{j,k}) \ \forall (j,k) \in J \}.$$

Bound $||p||_n \leq 2$ in the definition of \mathcal{P}_J holds because if $h = p + \tilde{h}$ for $h \in \mathcal{H}'_J$ and $\tilde{h} \in \tilde{\mathcal{H}}_J$, then $||p + \tilde{h}||_n \leq 1$ and $||\tilde{h}||_n \leq \tilde{\Omega}_{gr}(\tilde{h}) \leq 1$. Consequently,

$$H(u, \mathcal{H}(J), \|\cdot\|_n) \le H(u, \mathcal{H}'_J, \|\cdot\|_n) \le H(u/2, \mathcal{P}_J, \|\cdot\|_n) + H(u/2, \tilde{\mathcal{H}}_J, \|\cdot\|_\infty),$$
 (S5)

where we used the fact that the unit ball with respect to the $\|\cdot\|_{\infty}$ -norm is contained within the corresponding ball with respect to the $\|\cdot\|_n$ -norm. We note that \mathcal{P}_J is a ball of radis 2, with respect to the $\|\cdot\|_n$ -norm, in a linear functional space of dimension $\lesssim |J|+1$. Hence, $H(u/2,\mathcal{P}_J,\|\cdot\|_n)\lesssim |J|+|J|\log(1/u)$ by, for example, Corollary 2.6 in Van de Geer [2000]. Thus, the result of Lemma 1 follows from S5 if we also establish that $H(\delta,\tilde{\mathcal{H}}_J,\|\cdot\|_\infty)\lesssim |J|(1/\delta)^{2/m}$ for $\delta\in(0,1)$.

We complete the proof by deriving the stated bound on $H(\delta, \tilde{\mathcal{H}}_J, \|\cdot\|_{\infty})$. We represent $\tilde{\mathcal{H}}_J$ as

$$\Big\{\tilde{h}:\ \tilde{h}(\mathbf{x}) = \sum_{(j,k)\in J} \lambda_{(j,k)} g_{(j,k)}(x_{(j,k)}), \ \sum_{(j,k)\in J} |\lambda_{(j,k)}| \leq 1, \ g_{(j,k)} \in \mathcal{C}_2, \ \tilde{\Omega}(g_{(j,k)}) \leq 1, \ \|g_{(j,k)}\|_{\infty} \leq 1 \Big\}.$$

Given functions $\tilde{h}(\mathbf{x}) = \sum_{(j,k)\in J} \lambda_{(j,k)} g_{(j,k)}(x_j,x_k)$ and $\tilde{h}'(\mathbf{x}) = \sum_{(j,k)\in J} \lambda'_{(j,k)} g'_{(j,k)}(x_j,x_k)$ in $\tilde{\mathcal{H}}_J$, we have

$$\begin{split} \|\tilde{h} - \tilde{h}'\|_{\infty} & \leq \|\sum_{(j,k) \in J} \lambda_{(j,k)} g_{(j,k)} - \sum_{(j,k) \in J} \lambda_{(j,k)} g'_{(j,k)}\|_{\infty} + \|\sum_{(j,k) \in J} \lambda_{(j,k)} g'_{(j,k)} - \sum_{(j,k) \in J} \lambda'_{(j,k)} g'_{(j,k)}\|_{\infty} \\ & \leq \max_{(j,k) \in J} \|g_{(j,k)} - g'_{(j,k)}\|_{\infty} \sum_{(j,k) \in J} |\lambda_{(j,k)}| + \max_{(j,k) \in J} \|g'_{(j,k)}\|_{\infty} \sum_{(j,k) \in J} |\lambda_{(j,k)} - \lambda'_{(j,k)}| \\ & \leq \max_{(j,k) \in J} \|g_{(j,k)} - g'_{(j,k)}\|_{\infty} + \sum_{(j,k) \in J} |\lambda_{(j,k)} - \lambda'_{(j,k)}|. \end{split}$$

Consequently, if we let $\mathcal{G} = \{g : g \in \mathcal{C}_2, \ \tilde{\Omega}(g) \leq 1, \ \|g\|_{\infty} \leq 1\}$, let $\|\cdot\|_1$ denote the ℓ_1 -norm, and let B_1^d denote a unit ℓ_1 -ball in \mathbb{R}^d , then

$$H(\delta, \tilde{\mathcal{H}}_{J}, \|\cdot\|_{\infty}) < |J|H(\delta/2, \mathcal{G}, \|\cdot\|_{\infty}) + H(\delta/2, B_{1}^{|J|}, \|\cdot\|_{1}).$$

By the results in Birman and Solomjak [1967], $H(\delta/2, \mathcal{G}, \|\cdot\|_{\infty}) \lesssim (1/\delta)^{2/m}$. By the standard bounds on the covering numbers of a norm ball, $H(\delta/2, B_1^{|J|}, \|\cdot\|_1) \lesssim |J| + |J| \log(1/\delta)$. Consequently, $H(\delta, \tilde{\mathcal{H}}_J, \|\cdot\|_{\infty}) \lesssim |J| (1/\delta)^{2/m}$ for $\delta \in (0, 1)$.

S1.5 Proof of Lemma 2

We note that $||h||_n \leq r_n$ and $\tilde{\Omega}_{gr}(h) \leq 1$ for every $h \in \mathcal{H}(J)$. By Lemma 12 in the supplementary material for Tan and Zhang [2019] (cf. Corollary 8.3 in Van de Geer, 2000),

$$\sup_{h \in \mathcal{H}(J)} (\epsilon/\sigma, \mathbf{h})_n \lesssim n^{-1/2} \int_0^{r_n} \sqrt{H(u, \mathcal{H}(J), \|\cdot\|_n)} du + r_n \sqrt{t/n}$$
 (S6)

with probability at least $1 - e^{-t}$.

We note that $r_n = n^{-m/(2m+2)}$ and, thus, $n^{-1/2}r_n^{(m-1)/m} = r_n^2$. Using Lemma 1 to bound the entropy, we derive

$$n^{-1/2} \int_0^{r_n} \sqrt{H(u, \mathcal{H}(J), \|\cdot\|_n)} du \lesssim n^{-1/2} \int_0^{r_n} u^{-1/m} du \lesssim n^{-1/2} r_n^{(m-1)/m} = r_n^2.$$

Applying bound (S6), we conclude that

$$\sup_{h \in \mathcal{H}(J)} (\epsilon/\sigma, \mathbf{h})_n \lesssim r_n^2 + r_n \sqrt{t/n}$$

with probability at least $1 - e^{-t}$. The statement of the lemma is then a consequence of the fact that for every $f \in \mathcal{F}(J)$, function $f/[\|f\|_n r_n^{-1} + \tilde{\Omega}_{gr}(f)]$ falls in the class $\mathcal{H}(J)$.

S1.6 Proof of Lemma 3

Let M_s denote the number of distinct subsets of \mathcal{J} that have size M or smaller. We note that $\log(M_s) \leq 4M \log(ep)$ and, thus, $M_s e^{-t} \leq e^{4M \log(ep)-t}$. Applying Lemma 2 together with the union bound, we derive that, with probability at least $1 - e^{4M \log(ep)-t}$, inequality

$$(\epsilon/\sigma, \mathbf{f})_n \lesssim \left[r_n + \sqrt{t/n}\right] \|\mathbf{f}\|_n + \left[r_n^2 + r_n \sqrt{t/n}\right] \tilde{\Omega}_{gr}(f)$$

holds uniformly over $f \in \mathcal{F}_M$. We complete the proof by noting that for $t = 4M \log(ep) + \log(1/\epsilon)$ the above inequality becomes

$$(\epsilon/\sigma, \mathbf{f})_n \lesssim \left[r_n + \sqrt{\frac{\log(ep)}{n}} + \sqrt{\frac{\log(1/\epsilon)}{n}} \right] \|\mathbf{f}\|_n + \left[r_n^2 + r_n \sqrt{\frac{\log(ep)}{n}} + r_n \sqrt{\frac{\log(1/\epsilon)}{n}} \right] \tilde{\Omega}_{gr}(f),$$

and the corresponding lower-bound on the probability simplifies to $1 - \epsilon$.

S2 Definition of important Census/American Community Survey variables

S2.1 Definition of the variables in Figure 2

- Tot_Population_ACS_13_17: U.S.resident population includes everyone who meets the ACS residence rules in the tract at the time of the ACS interview.
- Prs_Blw_Pov_Lev_ACS_13_17: Number of people classified as below the poverty level given their total family or household income within the last year, family size, and family composition in the ACS population.
- College_ACS_13_17: Number of people ages 25 years and over at the time of interview with a college degree or higher in the ACS population.

- Not_HS_Grad_ACS_13_17: Number of people ages 25 years and over at time of interview who
 are not high school graduates and have not received a diploma or the equivalent in the ACS
 population.
- Pop_5_17_ACS_13_17: Number of persons ages 5 to 17 at the time of the ACS interview.
- Pop_18_24_ACS_13_17: Number of persons ages 18 to 24 at the time of the ACS interview.
- Pop_25_44_ACS_13_17: Number of persons ages 25 to 44 at the time of the ACS interview.
- Pop_45_64_ACS_13_17: Number of persons ages 45 to 64 at the time of the ACS interview.
- Pop_65plus_ACS_13_17: Number of persons age 65 and over at the time of the ACS interview.
- Hispanic_ACS_13_17: Number of people who identify as "Mexican", "Puerto Rican", "Cuban", or "another Hispanic, Latino, or Spanish origin" in the ACS population
- NH_White_alone_ACS_13_17: Number of people who indicate no Hispanic origin and their only race as "White" or report entries such as Irish, German, Italian, Lebanese, Arab, Moroccan, or Caucasian in the ACS population.
- NH_Blk_alone_ACS_13_17: Number of people who indicate no Hispanic origin and their only race as "Black,African Am.,or Negro" or report entries such as African American, Kenyan, Nigerian, or Haitian in the ACS population.
- ENG_VW_ACS_13_17: Number of ACS households where no one ages 14 years and over speaks English only or speaks English "very well".
- Othr_Lang_ACS_13_17: Number of people ages 5 years and over at the time of interview that speak a language other than English at home in the ACS population, regardless of ability to speak English.
- Diff_HU_1yr_Ago_ACS_13_17: Number of people who moved from another residence in the U.S. or Puerto Rico within the last year in the ACS population.
- Tot_Prns_in_HHD_ACS_13_17: All persons (household population) in ACS occupied housing unit. This is the numerator to calculate the average household size.
- Sngl_Prns_HHD_ACS_13_17: Number of ACS households where a householder lives alone.
- Female_No_HB_ACS_13_17: Number of ACS households with a female householder and no spouse of householder present.
- Rel_Child_Under_6_ACS_13_17: Number of ACS families with related children under 6 years old.
- Tot_Vacant_Units_ACS_13_17: Number of ACShousing units where no one is living regularly at the time of interview; units occupied at the time of interview entirely by persons who are staying two months or less and who have a more permanent residence elsewhere are classified as vacant.
- Renter_Occp_HU_ACS_13_17: Number of ACS occupied housing units that are not owner occupied, whether they are rented or occupied without payment of rent.
- Owner_Occp_HU_ACS_13_17: Number of ACS housing units where owner or co-owner lives in it.
- Single_Unit_ACS_13_17: Number of ACS housing units in which the structure contains only that single unit.
- Med_HHD_Inc_ACS_13_17: Median ACS household income for the tract.

- Med_House_Value_ACS_13_17: Median of ACS respondents' house value estimates for the tract.
- HHD_Moved_in_ACS_13_17: Number of ACS households where the householder moved into the current unit in the year 2010 or later.
- Occp_U_NO_PH_SRVC_ACS_13_17: Number of ACS housing units without a working telephone and available service.
- pct_HHD_No_Internet_ACS_13_17: Percentage of ACS households that have no Internet access.
- pct_HHD_w_Broadband_ACS_13_17: Percentage of ACS households that have broadband Internet access.
- pct_Pop_w_BroadComp_ACS_13_17: Percentage of people that live in households that have both broadband Internet access and a computing device of any kind in the ACS.
- pct_URBANIZED_AREA_POP_CEN_2010: The percentage of the 2010 Census total population that lives in a densely settled area containing 50,000 or more people.
- MrdCple_Fmly_HHD_ACS_13_17: Number of ACS households in which the householder and his or her spouse are listed as members of the same household; does not include same-sex married couples.
- NonFamily_HHD_ACS_13_17: Number of ACS households where a householder lives alone or with non-relatives only; includes same-sex couples where no relatives of the householder are present.
- MLT_U2_9_STRC_ACS_13_17: Number of ACS housing units in which the structure contains 2 or more housing units.
- MLT_U10p_ACS_13_17: Number of ACS housing units in which the structure contains 10 or more housing units.
- Civ_labor_16plus_ACS_13_17: Number of civilians ages 16 years and over at the time of the interview that are in the labor force in the ACS.
- Civ_emp_16plus_ACS_13_17: Number of civilians ages 16 years and over at the time of the interview that are unemployed in the ACS.
- One_Health_Ins_ACS_13_17: Number of people with one type of health insurance coverage in the ACS.
- Two_Plus_Health_Ins_ACS_13_17: Number of people with two or more types of health insurance coverage in the ACS.
- No_Health_Ins_ACS_13_17: Number of people with no health insurance coverage in the ACS.

S2.2 Definition of the variables in Figure 6(b)

- pct_Prs_Blw_Pov_Lev_ACS_13 _17: The percentage of the ACS eligible population that are classified as below the poverty level given their total family or household income within the last year, family size, and family composition.
- Age5p_German_ACS_13_17: Number of people ages 5 years and over who speak English less than "very well" and speak German at home in the ACS. Examples include Luxembourgian.
- pct_NH_White_alone_ACS_13_ 17: The percentage of the ACS population that indicate no Hispanic origin and their only race as "White" or report entries such as Irish, German, Italian, Lebanese, Arab, Moroccan, or Caucasian.

- pct_Owner_Occp_HU_ACS_13_17: The percentage of ACS occupied housing units with an owner or co-owner living in it.
- pct_Diff_HU_1yr_Ago_ACS_1 3_17: The percentage of the ACS population aged 1 year and over that moved from another residence in the U.S. or Puerto Rico within the last year
- pct_Vacant_Units_CEN_2010: The percentage of all 2010 Census housing units that have no regular occupants on Census Day; housing units with its usual occupants temporarily away (such as on vacation, a business trip, or in the hospital) are not considered vacant, but housing units temporarily occupied on Census Day by people who have a usual residence elsewhere are considered vacant.
- pct_College_ACS_13_17: The percentage of the ACS population aged 25 years and over that have a college degree or higher
- pct_Single_Unit_ACS_13_17: The percentage of all ACS housing units that are in a structure that contains only that single unit.
- pct_Sngl_Prns_HHD_Cen_2010: The percentage of all 2010 Census occupied housing units where a householder lives alone.
- pct_NH_Blk_alone_CEN_2010: The percentage of the 2010 Census total population that indicate no Hispanic origin and their only race as "Black, African Am., or Negro" or report entries such as African American, Kenyan, Nigerian, or Haitian
- pct_Tot_Occp_Units_ACS_13_17: The percentage of all ACS housing units that are classified as the usual place of residence of the individual or group living in it.
- pct_Not_HS_Grad_ACS_13_17: The percentage of the ACS population aged 25 years and over that are not high school graduates and have not received a diploma or the equivalent.
- pct_NoHealthIns1964_ACS_13_17: Percentage of people age 19 to 64 with no health insurance in the ACS.
- pct_US_Cit_Nat_ACS_13_17: The percentage of the ACS population who are citizens of the United States through naturalization.
- pct_NH_Asian_alone_Cen_2010: The percentage of the 2010 Census total population that indicate no Hispanic origin and their only race as "Asian Indian", "Chinese", "Filipino", "Korean", "Japanese", "Vietnamese", or "Other Asian".
- pct_Pop_25yrs_Over_ACS_13_17: The percentage of the ACS population who are ages 25 years and over at time of interview.
- pct_Not_MrdCple_HHD_Cen_2010: The percentage of all 2010 Census occupied housing units where no spousal relationship is present.
- Not_HS_Grad_ACS_13_17: The percentage of the ACS population aged 25 years and over that are not high school graduates and have not received a diploma or the equivalent.
- NH_White_alone_CEN_2010: Number of people who indicate no Hispanic origin and their only race as "White" or report entries such as Irish,German, Italian, Lebanese, Arab, Moroccan, or Caucasian in the 2010 Census population